

**Mechanism of Silicon Transfer in Tuyere Injected Reactors by
Carbothermic Reduction of Silica**

by

Ashish Agarwal

B.Tech., Indian Institute of Technology, Bombay (1996)

Submitted to the Department of Materials Science and Engineering
in Partial Fulfillment of the Requirements for the Degree of
Master of Science in Materials Science and Engineering

at the

MASSACHUSETTS INSTITUTE OF TECHNOLOGY

June 1998

©1998 Massachusetts Institute of Technology. All rights reserved

Signature of Author.....
Department of Materials Science and Engineering
May 8, 1998

Certified by.....
Uday B. Pal
John Chipman Associate Professor of Chemical Processing of Materials
Thesis Supervisor

Accepted by.....
Linn W. Hobbs
John F. Elliot Professor of Materials
Chairman, Departmental Committee on Graduate Students

MASSACHUSETTS INSTITUTE OF TECHNOLOGY
AUG 17 1998
LIBRARIES
ARCHIVES

Mechanism of Silicon Transfer in Tuyere Injected Reactors by Carbothermic Reduction of Silica

by

Ashish Agarwal

Submitted to the Department of Materials Science and Engineering on May 8, 1998
in Partial Fulfillment of the Requirements for the Degree of
Master of Science in Materials Science and Engineering

Abstract

The melting zone in a cupola has temperatures greater than 1773 K and a reducing atmosphere. This condition is suitable for the carbothermic reduction of silica. The key to the applicability of carbothermic reduction of silica for Ferro-alloy production is rapid in-situ production of SiC and its subsequent dissolution in the hot metal. The main objective of this investigation was to study the kinetics of the carbothermic reduction process and determine the optimum parameters for rapid and complete in-situ conversion of silica to SiC.

At temperatures above 1773 K the key reactions in the carbothermic reduction process are (1) $\text{SiO}_2(\text{s}) + \text{CO}(\text{g}) = \text{SiO}(\text{g}) + \text{CO}_2(\text{g})$, (2) $\text{SiO}(\text{g}) + 2\text{C}(\text{s}) = \text{SiC}(\text{s}) + \text{CO}(\text{g})$, (3) $\text{C}(\text{s}) + \text{CO}_2(\text{g}) = 2\text{CO}(\text{g})$. To meet the objective of this study, conditions must be such that the surface reactions occurring at the carbon and silica surfaces are rate limiting and the entire silica is converted to SiC. Pellet composition and structure in terms of carbon to silica ratio, their particle sizes and compaction pressure that ensure surface reaction is rate controlling, were determined. The gas-solid reaction kinetics was mathematically modeled in terms of the process parameters. It was observed that the reaction kinetics improved by reducing both carbon and silica particle sizes. However, below a certain critical particle size there was no significant improvement in the reaction kinetics. For complete conversion of SiO_2 to SiC, excess carbon and critical porosity are necessary to ensure that the entire $\text{SiO}(\text{g})$ generated by reaction (1) is consumed via reaction (2) within the pellet.

Thesis Supervisor: Uday B. Pal

Title: John Chipman Associate Professor of Chemical Processing of Materials

Table of Contents

1. Introduction	7
2. Theoretical Analysis	10
2.1 Thermodynamics	10
2.2 Kinetic Aspects.....	11
3. Reaction Mechanism	16
3.1 Experimental Setup.....	16
3.2 Results & Discussion	17
4. Thermogravimetry: Experimental Aspects	23
4.1 Experimental setup	23
4.2 Variable Reaction Parameters	24
5. Thermogravimetry: Results and Discussion	27
5.1 Kinetic Performance vs. Input Parameters	27
5.2 Kinetic Models	28
5.3 Effect of the gas atmosphere	30
6. Mathematical Modeling	46
6.1 Introduction	46
6.2 Development of the model	46
6.3 Results and Discussion.....	50
7. Conclusions	60
Nomenclature	61
Bibliography	63
Biographical Note	64

List of Figures

Figure 2.1	Equilibrium composition of chemical species as a function of C:SiO ₂ ratio.....	12
Figure 2.2	Equilibrium composition of chemical species as a function of temperature.....	13
Figure 2.3	Equilibrium composition of chemical species as a function of pressure.	14
Figure 2.4	Equilibrium partial pressures of the gaseous species.....	15
Figure 3.1	Schematic of the experimental setup to determine the reaction mechanism.....	20
Figure 3.2	Percentage reduction of SiO ₂ to SiO(g) for different compositions of the sample.....	21
Figure 3.3	Percentage conversion of SiO ₂ to SiC for different pellet compositions	22
Figure 4.1	Schematic representation of the experimental setup for thermogravimetry.....	26
Figure 5.1	Effect of C:SiO ₂ ratio on the reaction kinetics.	33
Figure 5.2	Effect of carbon particle size on the reaction kinetics.	34
Figure 5.3	Effect of silica particle size on reaction kinetics.	35
Figure 5.4	Effect of temperature on reaction kinetics.	36
Figure 5.5	Surface reaction model for different carbon sizes.	37
Figure 5.6	Ash layer model for different carbon sizes.	38
Figure 5.7	Surface reaction model for different C:SiO ₂ ratios.....	39
Figure 5.8	Ash layer model for different C:SiO ₂ ratios.....	40
Figure 5.9	Surface reaction model for different temperatures.	41
Figure 5.10	Ash layer model for different temperatures.....	42
Figure 5.11	Effect of CO partial pressure in the surrounding atmosphere on the reaction kinetics.	43
Figure 5.12	Estimation of the required CO pressures in the reaction pellet.	44
Figure 5.13	Effect of porosity on the reaction kinetics in presence of CO atmosphere.	45
Figure 6.1	Fractional conversion of carbon as a function of time for different carbon particle sizes.	54
Figure 6.2	Fractional conversion of silica as a function of time for different carbon particle sizes.	55
Figure 6.3	Fractional conversion of carbon as a function of time for different silica particle sizes.....	56
Figure 6.4	Fractional conversion of silica as a function of time for different particle sizes.	57

Figure 6.5 Fractional conversion of carbon as a function of time for different C:SiO₂ ratios.58
Figure 6.6 Fractional conversion of silica as a function of time for different C:SiO₂ ratios.....59

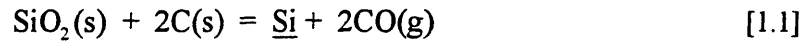
Acknowledgements

First of all I will like to thank my parents for providing me moral support and always encouraging me to achieve my goals. Then I will like to express my sincere gratitude to Prof. U.B. Pal for his valuable guidance, which helped me to conduct a successful study. I will like to thank the people in my research group, Dr. David Woolley, Mr. Prashant Sorai, Dr. Stephen Britten and Dr. Sridhar Seetharaman for making my stay at MIT a memorable one. I will also like to thank the department of Materials Science and Engineering for the excellent education and facilities it provided for my Master's program. I will like to take this opportunity to acknowledge my sponsors, Griffin Pipe Company for providing financial support for the project. I am also grateful to Prof. Alex Mclean from the University of Toronto for his helpful suggestions and input during the course of this work at MIT.

Chapter 1

Introduction

Silicon carbide is used as an alternate to the silicon dross in the production of ferrosilicon alloys^[1]. Silicon recovery improves if the silicon bearing raw materials are introduced directly into the superheated melting zone of a cupola. The melting zone of the cupola maintains conditions, which are suitable for the in-situ carbothermic reduction of silica. The overall reaction of interest is:



where $\underline{\text{Si}}$ represents silicon in solution in iron.

Possible products of carbothermic reduction that can react with Fe to give $\underline{\text{Si}}$ are $\text{SiO}(\text{g})$ and $\text{SiC}(\text{s})$. The reactions are:



Kinetics of reaction [1.2] is controlled by the transport of $\text{SiO}(\text{g})$ to the iron melt¹. As a consequence, the reaction is slow and the $\text{SiO}(\text{g})$ can escape or decompose without effectively reacting with carbon in the iron. On the other hand if the entire silica is rapidly converted to SiC , then it can easily alloy with the iron as shown in reaction [1.3]. Therefore, this study was focused on rapid and complete in-situ conversion of silica to SiC .

Many studies have been conducted to examine the kinetics of carbothermic reduction. Cutler et.al.^[3] investigated the kinetics of reduction of silica present in the rice husks in different CO

atmospheres. They found that the reaction between silica and carbon proceeds via the gas phases. The rate-controlling step for the formation of SiC is carbothermic reduction of silica to form SiO(g) and CO(g). They also found that reactions occurring at the carbon surface do play a role in controlling the reaction kinetics. Biernacki and Wotzak^[4] studied the kinetics of the reaction of one-to-one molar mixtures of crystalline silica and carbon powder in Ar and CO atmospheres. They found that though the reaction was predominantly controlled by chemical kinetics, it was influenced by diffusion mass transfer within the reacting bed of solids. Kimura et. al^[5] investigated the mechanism of reduction of silica graphite mixtures at temperatures between 1673 and 2073 K under argon atmosphere. The reduction products were both SiC and SiO(g). They reported that the production ratio of SiC increases significantly with increasing temperature and C:SiO₂ mixture ratio. In the early stage of reduction, the rate equation for interfacial reaction control is applicable to the reduction of SiO₂ with graphite. The rate-determining step is considered to be the chemical process at the surface of the graphite particles. When the reaction proceeds and a continuous layer of SiC is formed around the graphite particles, the rate of reduction shows a parabolic rate equation. The reduction of SiO₂ is controlled by the diffusion of carbon in SiC. Krstic^[6] synthesized submicrometer SiC (beta form) powders by reacting silica and carbon black at temperatures between 1723 K and 2073 K under vacuum. In this study it was found that the dominant mechanism above 1723 K is the reaction between gaseous SiO and C and that the rate of SiC formation is controlled by the rate of SiO formation. The objective of the present study was to determine the parameters in order to achieve surface reaction controlled kinetics for carbothermic reduction of silica and to ensure complete conversion of SiO₂ to SiC under conditions that exist in the melting zone of cupola. In other words obtain most rapid in-situ complete conversion of silica to SiC. A mathematical model was developed to simulate the experimental results for the surface reaction controlled kinetics and establish a clear theoretical understanding of the contributions of the different reactions taking place so that the results can be applied to a cupola.

Content of the remaining document is as follows: Chapter 2 discusses the thermodynamic and kinetic aspects of the reaction under different conditions. Chapter 3 deals with the preliminary experiments done using a horizontal tube furnace. These results along with the thermodynamic study were used to establish the reaction mechanism. Chapter 4 describes the experimental details of the thermogravimetry setup, which was used to study the reaction kinetics. Chapter 5 describes

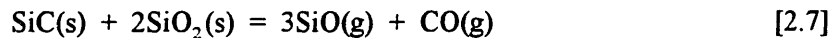
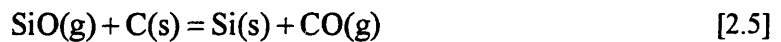
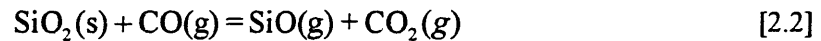
the analysis of the experimental results for the study of reaction kinetics thus obtained and discussion of the results. Chapter 6 describes in detail the mathematical model developed and compares the results with those obtained from the experiments. Chapter 7 concludes the present study.

Chapter 2

Theoretical Analysis

2.1 Thermodynamics

The possible reactions that could be taking place during carbothermic reduction of silica are:



Thermodynamic analysis was carried out using Outokumpu HSC chemistry software version 2.0 in order to determine the possible equilibrium phases involved in the reaction. Equilibrium phases are determined based on the calculation of Gibbs free energies of the individual phases^[6]. Fig.2.1 shows the equilibrium compositions as a function of the C: SiO₂ ratio of the starting mixtures at a temperature of 1873 K. It can be seen that for C:SiO₂ ratios greater than 3, SiO(g) is negligible and SiC and CO(g) are the dominant reaction products. Fig.2.2 shows the equilibrium compositions of various chemical species as a function of temperature with a starting C:SiO₂ ratio of 3:1. It is seen that the SiC formation begins at a temperature of about 1773 K. Also, above 1823 K the stable phases are SiC and CO(g). Pressure in the melting zone also varies. Fig.2.3 shows the equilibrium compositions of various chemical species as a function of the system

pressure. Below a pressure of 2 atm SiC and CO(g) are the stable products of the reduction reaction.

2.2 Kinetic Aspects

Thermodynamic analysis shows that SiC and CO(g) are the dominant reduction products for C:SiO₂ ratio greater than 3:1 and temperatures over 1823 K. However, SiO(g) has some equilibrium partial pressure and it increases with temperature (fig.2.4). As a result, some SiO(g) can leave the C-SiO₂ mixture (pellets) used for in-situ carbothermic reduction. As stated earlier the kinetics of the reaction



is controlled by the transport of SiO(g) to the iron melt¹. As a consequence significant quantities of SiO(g) can escape to the upper zones of cupola and get wasted. Objective is to achieve maximum conversion of SiO(g) to SiC within the C-SiO₂ mixture (pellets) and transfer it to the iron melt. This is possible by reaction [2.3] and the following reaction:



Reaction kinetics should be such that maximum conversion of silica to SiC takes place in the least possible time.

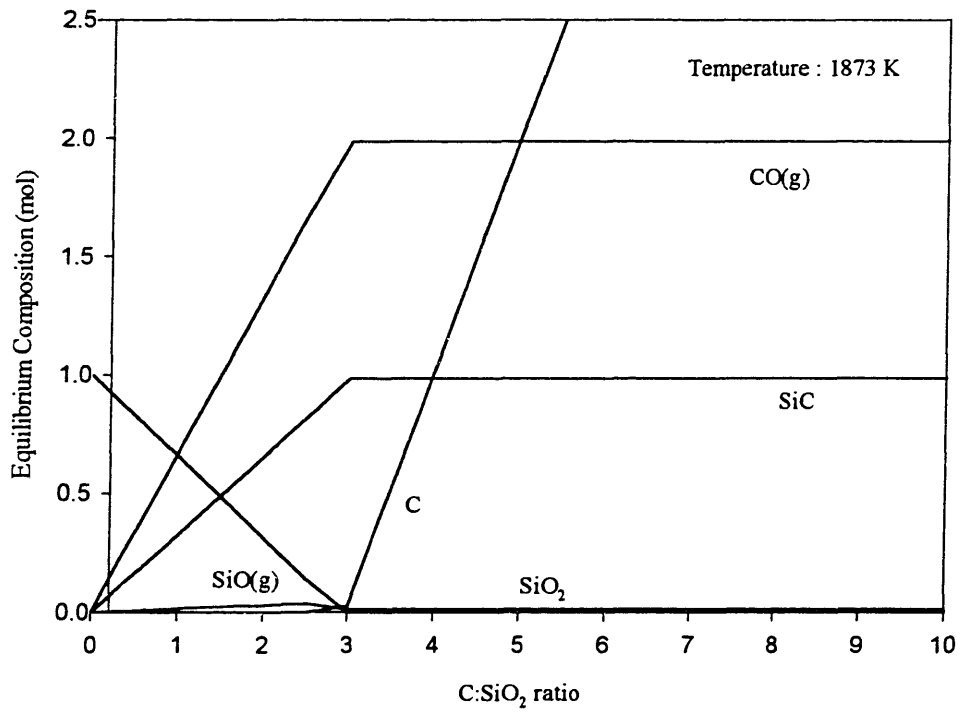


Fig 2.1 Equilibrium composition of chemical species as a function of C:SiO₂ ratio.

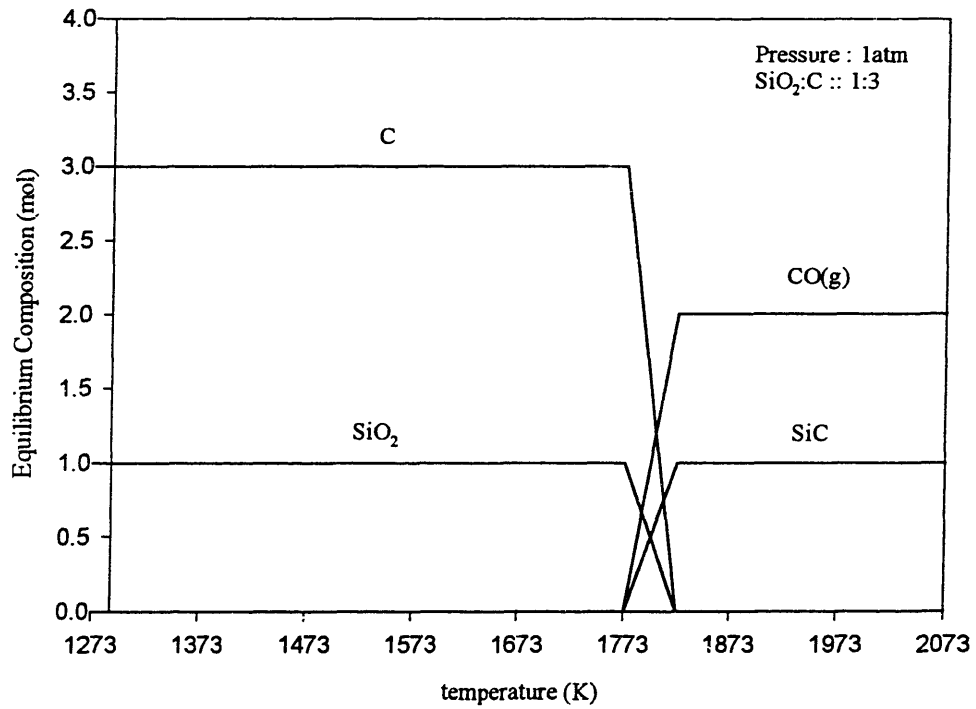


Fig 2.2 Equilibrium composition of chemical species as a function of temperature.

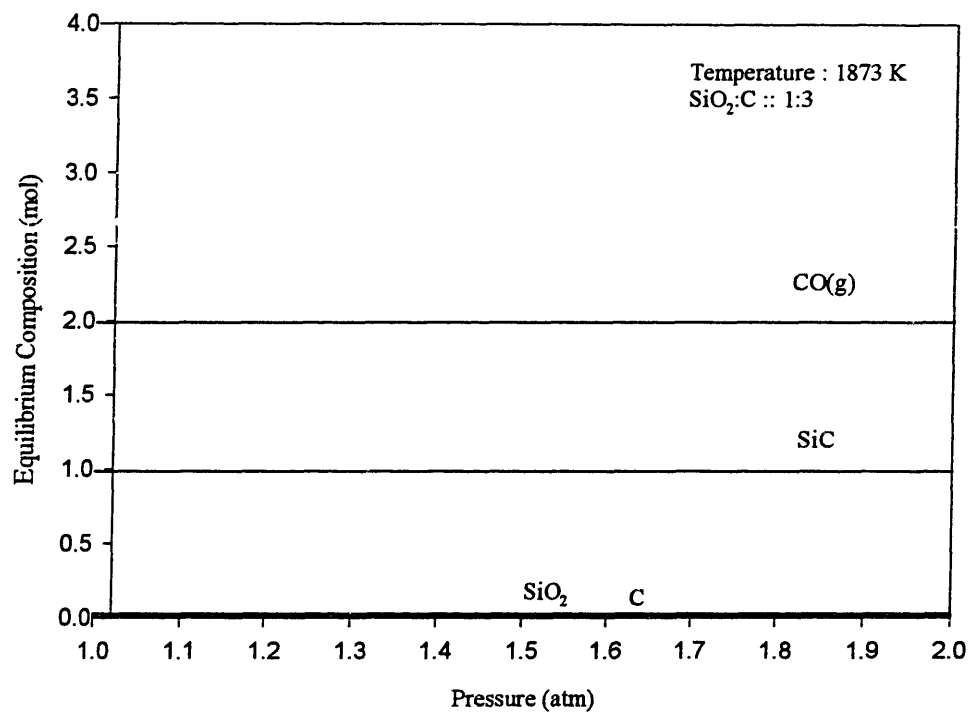


Fig 2.3 Equilibrium composition of chemical species as a function of pressure.

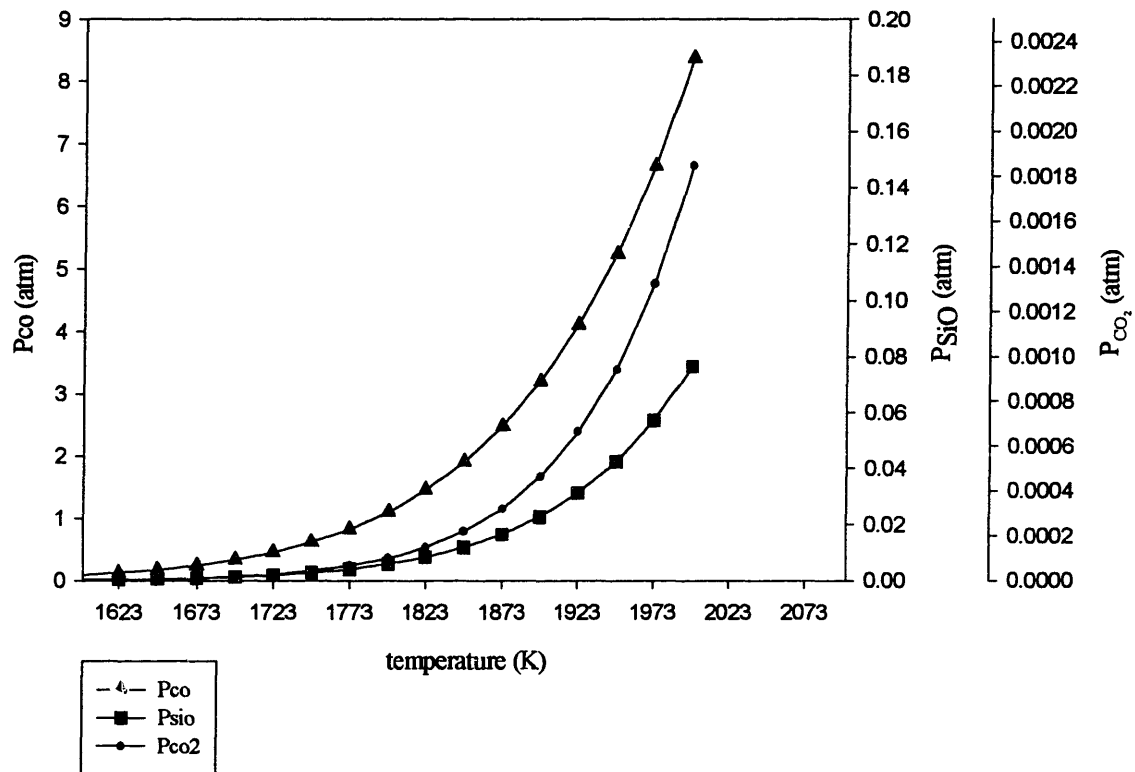


Fig 2.4 Equilibrium partial pressures of the gaseous species.

Chapter 3

Reaction Mechanism

In order to control the reaction kinetics it is essential to understand the reaction mechanism involved. A series of experiments were conducted to determine the possible reactions involved in the carbothermic reduction under conditions similar to those existing in the melting zone of the cupola. Using the results of chemical analysis of the products, a reaction mechanism was established. The effect of different compositions of the starting materials on the extent of conversion of silica to SiC was studied. The C:SiO₂ ratio required for making the reaction surface limited was identified. These results were used to determine the chemical composition of the pellets needed for thermo-gravimetric study to be described later.

3.1 Experimental Setup

Experimental setup is shown in figure 3.1. Reaction chamber was an open ended alumina tube of 1.25" diameter. A Lindberg / blue M resistance furnace was used to achieve the desired temperature. Tube was sealed at both ends to make it gas tight. Argon was used as the purge gas. Gas flow was controlled by rotameters. Gas from the reaction chamber was fed to an electronic Omega mass flowmeter, which in turn fed the gas to Anarad infra red CO gas analyzer. Gas analyzer was calibrated using a certified 20% CO-N₂ gas mixture. A supplementary gas source was also used as the gas analyzer pump was designed to draw gas at the rate of 2 litres/min. In the later experiments this was taken care of by using a rotameter right before the gas analyzer in the flow chain for the gas. Voltage signals from the mass flowmeter and the gas analyzer were fed to a data acquisition system, Fluke hydra logger and the corresponding data was stored in a Dell 80486 computer. Temperature of the hot zone was monitored by a B type thermocouple.

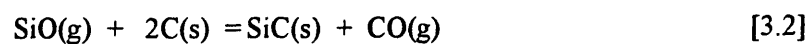
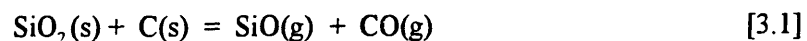
Carbon black (68 nm) and silica (10 μ) were mixed in the desired ratio in a ball mill using silica beads for about 12 hrs. Powders were pressed into pellets of diameter 0.75" and weighing 1.2

grams using a pressing load of about 9000 psi. The pellet was placed in an alumina boat in the cold zone of the horizontal tube furnace and the furnace tube was purged with argon. The furnace tube was heated to 1873 K and the boat was pushed into the hot zone with an alumina rod. CO evolution was detected and measured by an infrared gas analyzer. When no more CO evolution was detected, the boat was pushed out of the hot zone and cooled in the argon atmosphere. Weight loss was measured. Phase analysis in the samples was done using a Rigaku IU300 DMAX-B wide-angle diffractometer. Samples were sent out to LECO technical services laboratory where these were analyzed for the carbon and oxygen content using combustion test with model CS-444. . Experiments were repeated by varying the flow rate of argon from 30 ml/min to 300 ml/min. and also by varying the C:SiO₂ ratio while keeping the flow rate fixed.

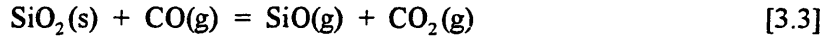
3.3 Results & Discussion

Mechanism

Whiskers were observed on the sides of the alumina boat for low flow rates for pellets with C:SiO₂ ratio of 3 or less. XRD analysis indicated that the phase present was cristobalite (SiO₂). However, no silicon was detected. Presence of SiO₂ whiskers indicates that SiO(g) is one of the reaction products. For higher flow rates SiO(g) generated was driven out of the system by the flow of the purge gas. XRD analysis of the pellets revealed the presence of SiC, C and trace amount of SiO₂. SiC forms a layer around carbon particles. Si in SiO(g) or C then has to diffuse through the SiC layer for further reaction to take place. This transport process is very slow^[5] and as a result some SiO(g) leaves the C-SiO₂ pellet. Diffusion coefficients of Si and C are too low for solid–solid reaction to be the dominant mechanism^[5]. It can therefore, be classified as a gas-solid reaction. In the given time frame, this eliminates the possibility of significant reaction between SiC and retained SiO₂. Also SiC formation on the surface of carbon particles has been reported^[5]. Possible reaction steps are:

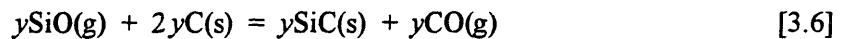
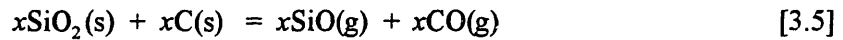


Reaction [3.1] acts as the initiation step. However, as soon as some reaction takes place a large quantity of CO(g) is liberated which suppresses any further reaction due to large partial pressure of CO(g) (2.42 atm at 1873 K). Also, reaction [3.1] takes place at the points of contact between SiO₂ and C particles. As a result, the contact breaks as soon as some reaction takes place. Propagation of this reaction can take place only in the gas-solid mode. Possible steps are:

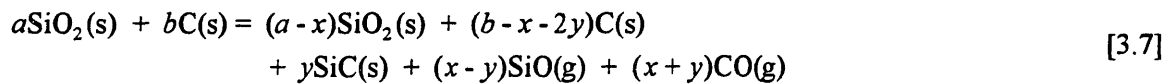


Quantitative Analysis

Quantitative analysis was done using the mass balance principles. CO evolution was estimated by calculating the area of the CO flow rate vs. time plots generated from the data of the gas analyzer. Combustion analysis of the pellets gave the C and O content of the samples. Oxygen content corresponds to the retained silica while carbon content corresponds to the SiC and retained carbon in the system. Total weight loss measured by an electronic balance, can be attributed to the CO(g) and SiO(g) evolution. The net reaction can then be written in the following manner:



Let us assume that initially we have a moles of SiO₂ and b moles of C. Then the overall reaction can be represented in the following manner:



Knowing the oxygen content of the reacted pellets we can find out the amount of retained silica. This will give us the value of x in the above equation. Using this value and the carbon content of the pellet, value of y can be estimated. These values can be verified against the total CO evolution

measured separately using the gas analyzer. Usually an error less than 10% was found in the above quantitative analysis.

Effect of initial pellet composition

It was observed that some $\text{SiO}(\text{g})$ leaves the C-SiO_2 pellet when stoichiometric amounts ($\text{C}:\text{SiO}_2$ ratio of 3) are used. In order to study the chemical kinetics using thermogravimetry it was essential to completely react the $\text{SiO}(\text{g})$ generated and convert it to SiC so that the weight loss could be correlated only to the $\text{CO}(\text{g})$ evolution. A higher $\text{C}:\text{SiO}_2$ ratio of 5:1 was used for this purpose. Quantitative analysis was done as stated above. More SiO_2 was reduced to $\text{SiO}(\text{g})$ for higher $\text{C}:\text{SiO}_2$ ratio.(fig 3.2). Also, a significantly higher conversion to SiC (close to 95%) was achieved for higher $\text{C}:\text{SiO}_2$ ratio.(fig.3.3). For a given particle size of carbon, larger surface area is available for higher $\text{C}:\text{SiO}_2$ ratios and this enhances the surface reaction kinetics for reaction [3.2]. This ensures a more complete conversion of $\text{SiO}(\text{g})$ to SiC .

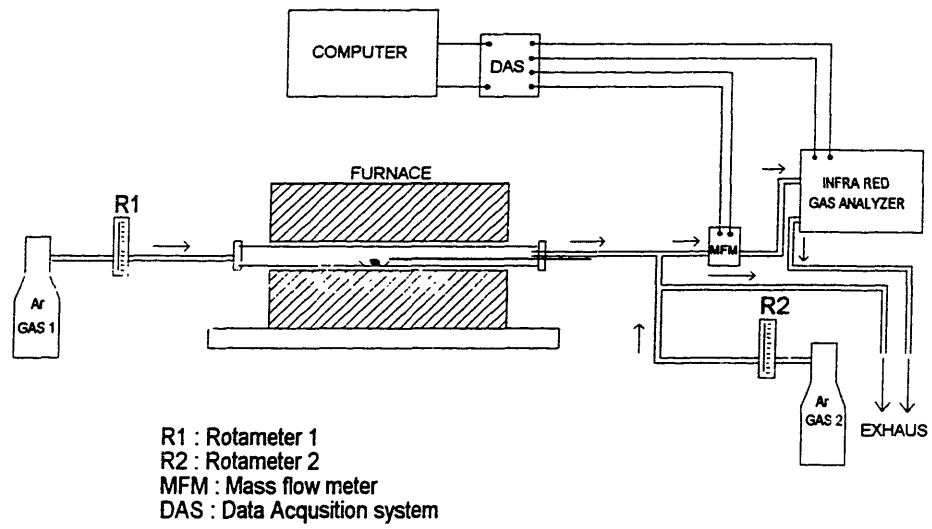


Figure 3.1 Schematic of the experimental setup to determine the reaction mechanism.

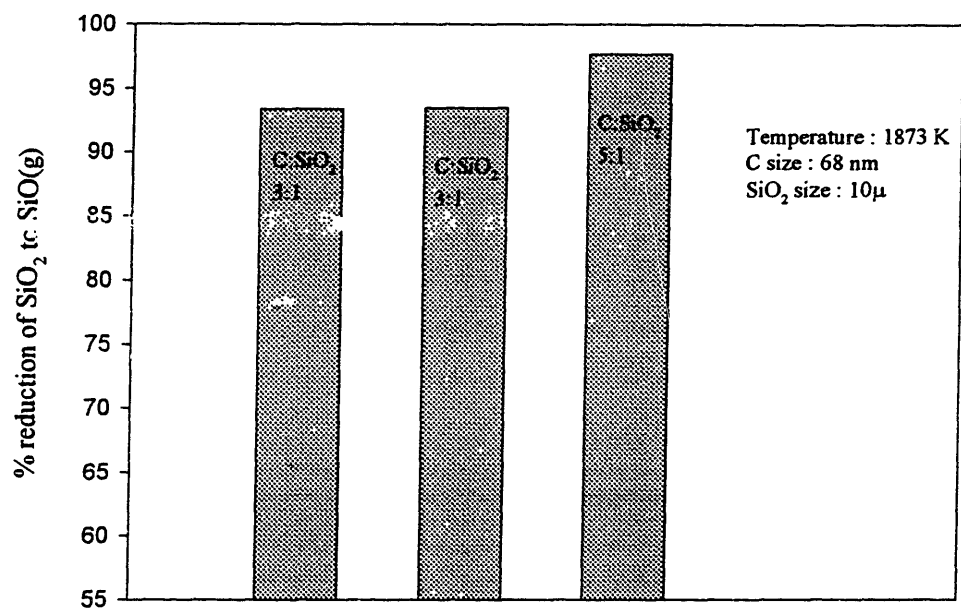


Figure 3.2 Percentage reduction of SiO₂ to SiO(g) for different compositions of the sample.

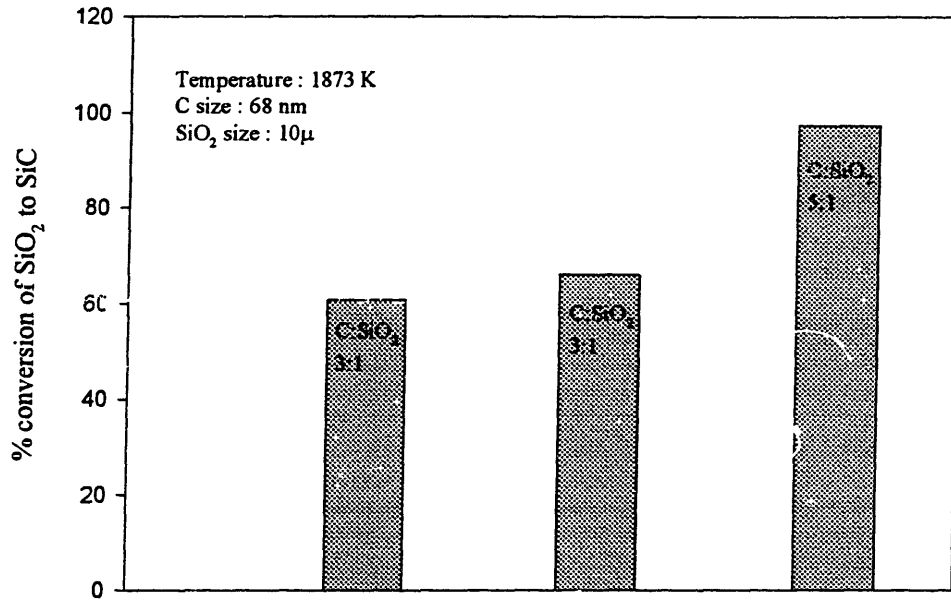


Figure 3.3 Percentage conversion of SiO₂ to SiC for different pellet compositions.

Chapter 4

Thermogravimetry: Experimental Aspects

Since, the present study involved evolution of CO(g) as the reaction product, it was possible to follow the reaction as a function of time by measuring sample weight change. This is possible only when all SiO(g) that is generated is consumed by the carbon particles in the C-SiO₂ pellet. This was ensured by using the starting C:SiO₂ ratio of at least 5:1. Some experiments were conducted using a C:SiO₂ of 3:1 in order to study the effect of C content of the samples on the reaction kinetics. The reaction rate obtained in this case was a result of small amount of SiO(g) evolution along with the CO(g) evolution and therefore cannot be directly compared with the rate obtained for pellets that contained higher amounts of carbon and resulted only in CO(g) evolution. However, they can be compared qualitatively keeping this fact in mind. In this chapter the experimental aspects have been described in detail. Results and discussion are presented in the following chapter.

4.1 Experimental setup

Schematic of the experimental setup is shown in fig.4.1. High temperature D101-02 AT Cahn balance was used for thermogravimetry. The microbalance is rated for a maximum sample weight of 100 grams. In this setup, the sample was stationary as it had to be suspended from the balance. In order to study the reaction kinetics it was necessary to subject the sample to the hot zone instantaneously. To achieve this the furnace was made mobile instead. An Oslon lift was used for this purpose. The CM resistance furnace was lowered and raised by using a mechanical winch. Alumina tube could not be used as a furnace tube because higher thermal shock resistance was desired. So a closed end mullite tube (2.25" OD x 24" length) was used as the reaction chamber. Initially the temperature profile of the furnace was measured. This was used to determine the relative positions of the furnace and the reaction tube in the situations when the sample was supposed to be in the cold zone and when it was supposed to be in hot zone. Cold zone can be

defined as the furnace zone having a temperature such that no reaction or minimal reaction occurs between the reactants, carbon and silica in our case. From the thermodynamic analysis it was found that the maximum allowable temperature for the cold zone is 1573 K. Hot zone is the furnace zone having the temperature desired for studying the reaction kinetics.

Hangdown assembly consisted of a hand made platinum chain attached to an alumina rod and an alumina crucible suspended from the other end of the alumina rod. Alumina crucible was used to hold the samples. This configuration was used to prevent the assembly from breaking due to thermal shock while running the experiments. Other end of the platinum chain was connected to the hook on the sample side of the Cahn balance.

Nozzles were provided in the mullite tube to maintain a continuous flow of the gas. To ensure that the gas flow direction was one way only, gas was transmitted by means of a small diameter mullite tube attached to the inlet of the reaction chamber right to the bottom and then released. This gas rose in the reaction chamber and escaped from the outlet. Also, the balance was purged continuously with argon to prevent the flow of gases into the balance chamber. Care was taken to avoid the effect of buoyancy on the weight changes due to accumulation of the gas in the reaction chamber. Gas from the reaction chamber was fed to an electronic Omega mass flowmeter, which in turn fed the gas to Anarad infra red CO gas analyzer used in the horizontal tube experiments. Gas flow was controlled by rotameters. Voltage signals from the mass flowmeter and the gas analyzer were fed to a data acquisition system, a Fluke hydra logger and the corresponding data was stored in a Dell 80486 computer. Balance was connected to a control unit, which fed the data to the computer. Balance was calibrated by using NIST standard weights. It was then tared to account for the weight of the hangdown assembly. Dome cap was sealed to make it gas tight.

Carbon and silica were mixed in a predetermined ratio in a ball mill using silica beads for about 12 hrs. Powders were pressed into pellets of diameter 0.75" and weighing 1.2 grams using a pressing load of about 9000 psi. Samples were suspended from the balance in an alumina crucible by means of the hangdown assembly and were enclosed in the mullite tube. Furnace was preheated to the desired temperature and was raised so that the sample was in the hot zone. Temperature of the hot zone was measured by a B-type thermocouple, which was located outside the reaction tube. There was a lag of about 3-4 minutes before the reaction started. This was the

time needed for the sample to reach the desired temperature. As the reaction proceeded, the weight loss due to CO(g) evolution was recorded by the balance. When no more weight loss was recorded, the furnace was lowered so that the sample was in the cold zone. Flow rate of the purge gas (argon) was maintained at 200 ml/min. Weight loss for the reacted sample was measured using an electronic balance and the result was compared with the final weight loss data obtained from Cahn balance. Difference in the weight loss measurements was found to be less than 5%. Gas analyzer served as a detector of CO(g) in these set of experiments. Phase analysis in the reacted samples was done using a Rigaku IU300 DMAX-B wide-angle diffractometer. Jandel Scientific SigmaPlot Software version 3.0 was used to analyze the data and make relevant plots. Apart from the chemical composition (C:SiO₂ ratio) other variable parameters taken into consideration were carbon particle size, silica particle size, temperature and porosity. Control experiments were conducted by varying one of the above parameters while keeping other inputs fixed. Experiments were also conducted to study the effect of the gas atmosphere on the reaction kinetics.

4.2 Variable Reaction Parameters

C:SiO₂ ratios used were 3:1, 5:1 and 10:1. Three different carbon particle sizes were used: 68nm (carbon black), 20 μ and 75 μ (graphite). It is known that different forms of carbons have different reactivity. However, this was not taken into consideration in the present study. Variable silica particle sizes were 10 μ , 20 μ and 200 μ silica from Alfa AESAR. Reaction kinetics were studied at the temperatures of 1723, 1798 and 1873 K. In all the above experiments argon was used as the purge gas. Actual atmosphere inside the tuyere zone of the iron cupola is 100% CO(g). A set of experiments was conducted to study the effect of outside atmosphere on the reaction kinetics. Atmospheres used were Ar, 10% CO+ Ar, 20% CO+ Ar, 20% CO +N₂ and 100% CO.

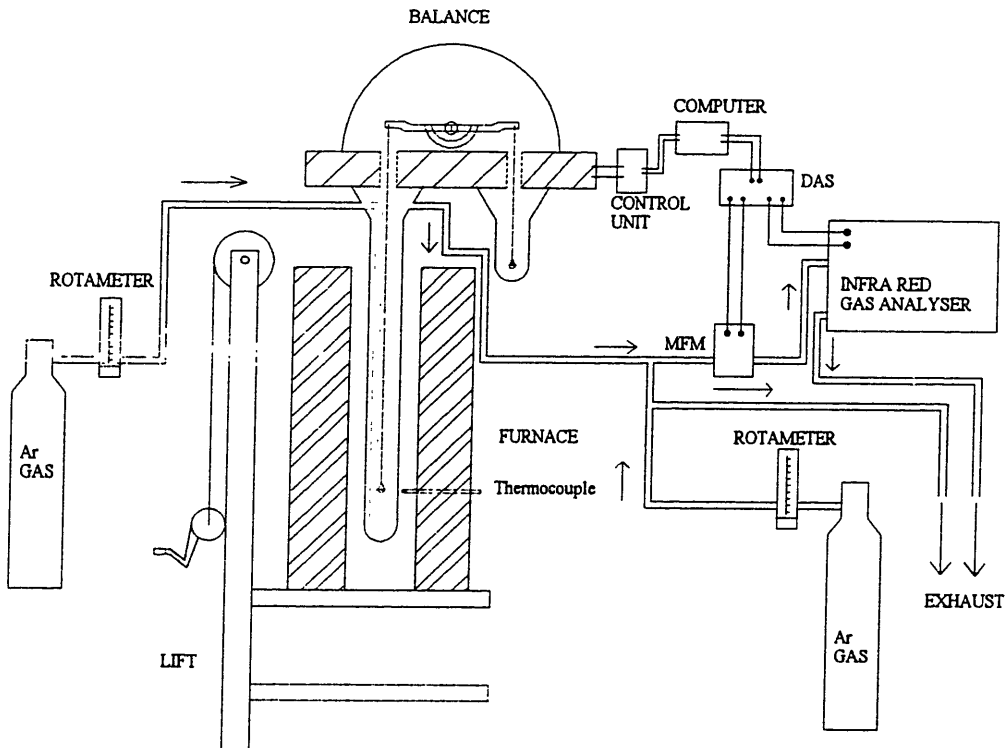


Figure 4.1 Schematic representation of the experimental setup for thermogravimetry.

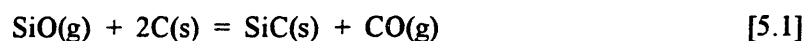
Chapter 5

Thermogravimetry: Results and Discussion

5.1 Reaction Kinetics vs. Input Parameters

Effect of initial pellet composition

For a given particle size of SiO₂ and C, the carbon content of the samples influences the rate of CO evolution as can be observed in fig.5.1. Weight loss has been normalized with respect to the starting amount of silica present in the pellet. Initially the kinetics is same for all the starting C:SiO₂ ratios. However, as the reaction proceeds less and less carbon surface area becomes available which reduce the kinetics for following reactions occurring on the carbon surface:



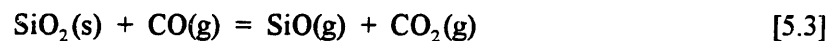
This is especially true for the samples with lower C:SiO₂ ratios leading to lower overall kinetics.

Effect of carbon particle size

Also, for a given C:SiO₂ ratio and a given SiO₂ particle size, the reaction rate increases with decrease in the carbon particle size (fig.5.2). This can be attributed to the higher carbon surface area available for the smaller particle size, which enhances the kinetics for reactions [5.1] and [5.2]. However, it was observed that below a critical particle size the kinetics was not significantly affected. Thus, reaction kinetics for particle sizes of 20μ and 68nm are not very different though the size difference is significant.

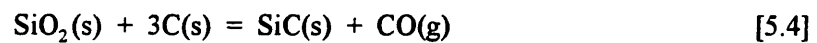
Effect of silica particle size

Fig.5.3 shows the effect of silica particle size on the reaction kinetics for a given C:SiO₂ ratio and a given C particle size . It was observed that reaction kinetics is not affected significantly below a certain critical size of the silica particles. For larger sizes, the reaction kinetics increases with a decrease in the silica particle size. This can be attributed to the increase in the available surface area of silica, which leads to an increase in the kinetics of the following reaction occurring on the silica surface:



Effect of temperature

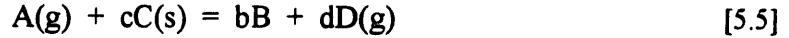
Reaction kinetics increases with increase in temperature for a given C:SiO₂ ratio and a given particle size of C and SiO₂ (fig.5.4). Thermodynamically, the overall reaction



is endothermic and is favored at high temperatures. If we consider the individual reactions then reactions [5.2] & [5.3] are endothermic whereas reaction [5.1] is exothermic. However, the equilibrium constant for reaction [6] is very high^[7]. Thus, a rise in temperature drives the carbothermic reduction in the forward direction.

5.2 Kinetic Models

In a powder compact where the reaction occurs between solids through gaseous intermediates, the possible reaction controlling steps could be surface reactions, diffusion of the gaseous reactants and products through the ash (product) layer or diffusion of the gases through the pores or a combination of these. Usually, diffusion through the gas film surrounding the particles is not rate limiting because the transport distances within the compact are small. A typical gas-solid reaction can be represented by the following equation:



B can either be a solid or a gas. In either case, when surface reaction is the rate-controlling step, fractional conversion of solid C can be represented by the following equation^[8]:

$$\left[1 - (1 - X_c)^{1/3}\right] = \frac{K_1 t}{r_c} \quad [5.6]$$

where X_c is the fractional conversion of solid C, t is the time, r_c is the original particle size of solid C and K_1 is a constant representing the intrinsic rate.

If B is a solid then the diffusion of A(g) and D(g) through the porous layer of B can also be rate limiting. In that case the conversion of solid C can be written as^[8]:

$$\left[1 - \frac{2}{3} X_c - (1 - X_c)^{2/3}\right] = \frac{K_2 t}{r_c^2} \quad [5.7]$$

where K_2 is a constant representing the diffusivity of gaseous reactants

For the conversion of carbon both models can apply as the gasification of carbon through the Boudouard reaction and the formation of porous SiC layer are occurring simultaneously. In case of silica particles only gasification is involved and the surface reaction model should apply.

The following assumptions were made while applying these models in the present study:

- (1) The concentration of gaseous species is uniform throughout the pellet.
- (2) The system is isothermal.

This would be the case for a system of uniformly mixed, fine particles and small size of the pellets. Also the reactions were assumed to be irreversible and of the first order. These models were tested for the conversion of carbon particles in the context of different input parameters discussed above. Linear relationship between the model expression for conversion of the solid and time can confirm the applicability of the model. Fractional conversion X_c was computed as the fraction of C reacting with time to generate CO(g) and leading to a subsequent weight loss.

Fig.5.5 shows the plots of the surface reaction model expression for conversion of carbon against time for different sizes of carbon particle. Initially there is a lag of 3-4 minutes, which can be attributed to the heating time required for the sample. For most part of the reaction, the plots are linear indicating that the surface reaction model holds. The plots for ash layer model are non-linear indicating that the diffusion through the SiC layer is not rate limiting (fig.5.6). Figs.5.7 and 5.8 show the effect of C:SiO₂ ratio. For a C:SiO₂ ratio greater than 5, surface reaction model holds. However, for a C:SiO₂ ratio of 3:1 surface reaction model does not hold for the later stages of the reaction. For this stoichiometric ratio, no extra carbon surface is available for the reaction. As the SiC layer around the carbon particles builds up, diffusion of the gases through this layer becomes rate limiting and it also causes some of the SiO(g) to escape from the pellet without reacting with carbon. For a C:SiO₂ ratio of 5:1, surface reaction model is applicable for the range of temperatures considered (figs. 5.9 and 5.10).

In this section it has been demonstrated that C:SiO₂ ratios higher than 5:1 are needed for the surface reaction model to be applicable for the particle sizes and pellet structures considered. It was shown earlier that this also resulted in complete conversion of silica to SiC. If a larger carbon particle size is used higher C:SiO₂ ratios are needed to ensure that surface reaction kinetics is rate determining. The individual contributions of the key reactions involved in the carbothermic reduction of silica in the pellet when surface reaction is rate controlling, have been mathematically modeled and are explained in chapter 6.

5.3 Effect of the gas atmosphere

Above experiments were carried out in an argon atmosphere. However, the hot melting zone of cupola has a reducing atmosphere primarily comprising of CO(g). Fig.5.11 shows the effect of different atmospheres on the reaction kinetics. As the CO content of the purge gas increases the reaction kinetics decrease. Also, after the completion of the reaction a higher weight loss was observed. Some silica whiskers were observed in the cooler parts of the reaction tube. Thus, the excess weight loss can be attributed to some SiO(g) loss from the system. Possible explanation for these observations is as follows: At the microscopic level, as soon as the SiO(g) reacts with the C, a large amount of CO(g) is generated. CO(g) partial pressure P_{CO} rises to the equilibrium value and the reaction stops. This CO(g) has to effuse out of the pellet for further reaction to take

place. Effusion of CO(g) can take place by diffusion mechanism as well as by Darcy flow. The effusion flow rate of CO(g) can then be represented as ^[9-11]

$$V_o = \frac{1}{4.2} \frac{\varepsilon^3}{(1-\varepsilon)^2} \frac{\Delta P}{L \eta_{CO} S_o^2} + \frac{2 D_{eff-CO}}{\rho_{CO} RT} \frac{\Delta P_{CO}}{L} \quad [5.8]$$

transport due to Darcy flow transport due to concentration gradient

V_o is the superficial velocity of the CO(g), L is the half thickness of the pellet. η is the viscosity of the gas, S_o is the particle surface area per unit volume of the solid, ε is the porosity, ρ is the molar density of CO(g), D_{eff-CO} is the effective diffusivity of the gas and ΔP is the required pressure difference.

V_o was estimated at different times during the reaction using weight loss data recorded during thermogravimetry experiments using Ar as the purge gas. This effusion flow rate for a given particle size was used as a basis to calculate the P_{CO} that would be required to get similar kinetics in CO atmosphere for the same particle size. Both knudsen diffusivity and molecular diffusivity were taken into consideration in determining the effective diffusivity D_{eff-CO} . Molecular diffusivity and viscosity η was estimated using Chapman Enskog theory^[10]. S_o and ε were estimated theoretically by taking into consideration the particle sizes of carbon and silica and making an assumption that the particles are uniform spheres. Value of ε was estimated to be 0.4. The value for tortuosity τ was chosen as 2.0 ^[9,12]. Half thickness L of the pellet was estimated to be 2mm.

Fig.5.12 shows the equilibrium P_{CO} and the required CO(g) partial pressure for CO effusion for different particle sizes of carbon at different points of time during the reaction in CO atmosphere. Different times are represented by the fractional conversion of carbon x_c . Calculated P_{CO} within the pellet for reaction in Ar atmosphere is also shown for different carbon particle sizes.. As the equilibrium partial pressure of CO(g) is much higher than the required pressure, the overall rate should be unaffected by the effusion of CO(g). However, in 100% CO(g) atmosphere the required P_{CO} for CO(g) effusion increases. Though the equilibrium P_{CO} is still higher than the required P_{CO} , it is possible that the actual average P_{CO} is only slightly greater than atmospheric pressure. In that

case, having CO(g) at 1 atm pressure as the purge gas will lead to lower driving force for CO(g) effusion and hence, a lower chemical kinetics.

Fig.5.13 shows the effect of porosity on the reaction kinetics. We can see that the reaction kinetics improve for the loose bed of powder mixtures which obviously has a higher porosity than the pellet. The diffusivity of CO(g) increases with porosity which leads to a higher rate of CO effusion from the pellet and hence, an increase in reaction kinetics.. However, a higher total weight loss was observed due to SiO(g) leaving the system. The diffusivity of SiO(g) also increases with porosity which leads to a higher rate of SiO(g) effusion from the pellet. This indicates that the chemical kinetics for the reduction of SiO₂ to SiO(g) is at least comparable to the kinetics of reaction(s) occurring on the carbon surface. It also demonstrates the importance of porosity in retaining the SiO(g), and ensuring complete conversion to SiC apart from controlling the carbothermic reduction kinetics.

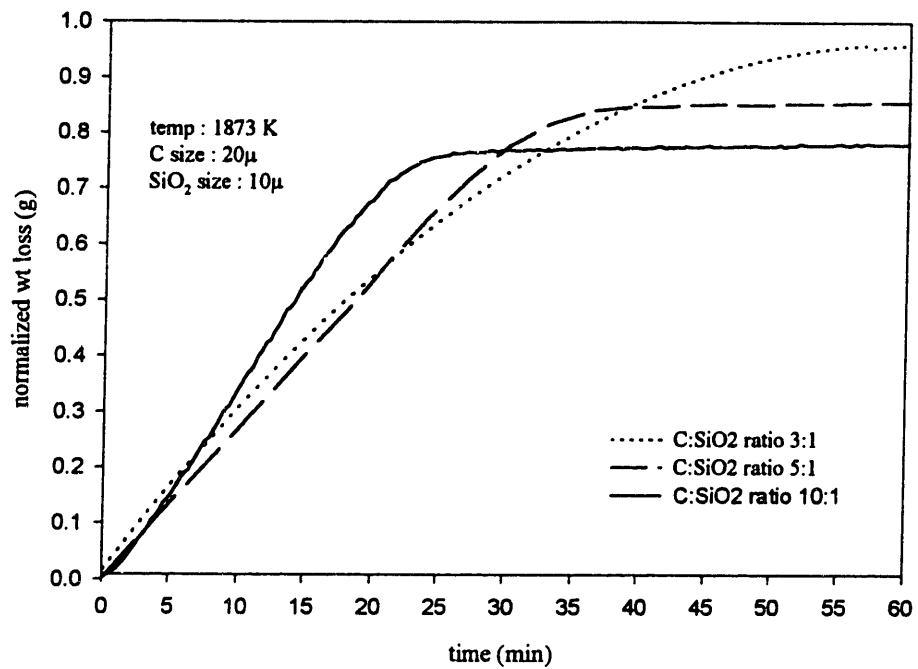


Figure 5.1 Effect of C:SiO₂ ratio on the reaction kinetics.

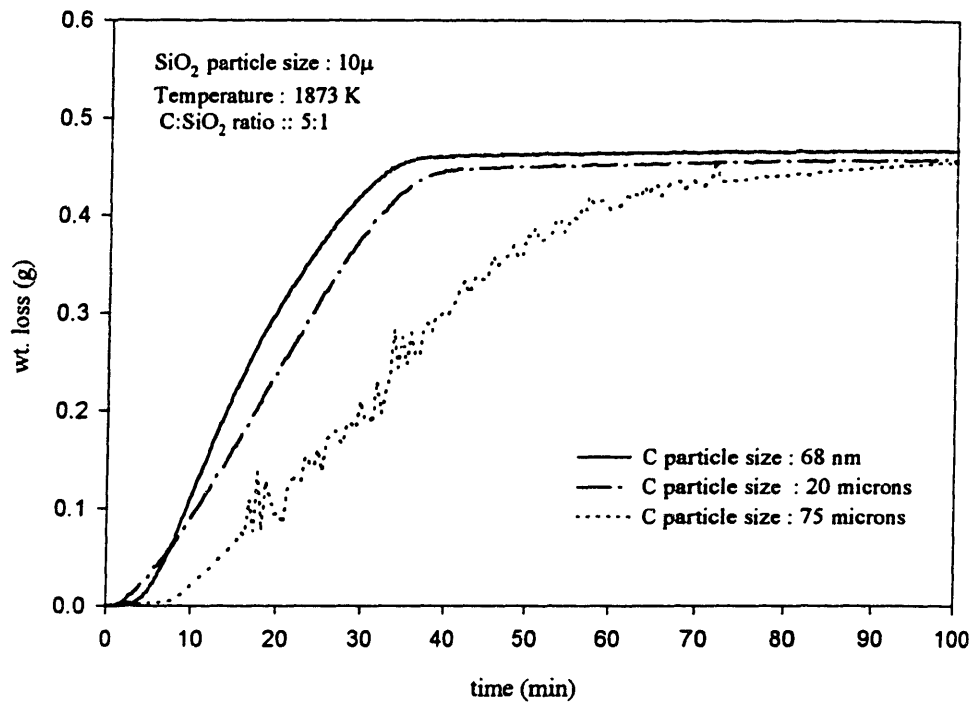


Figure 5.2 Effect of carbon particle size on the reaction kinetics.

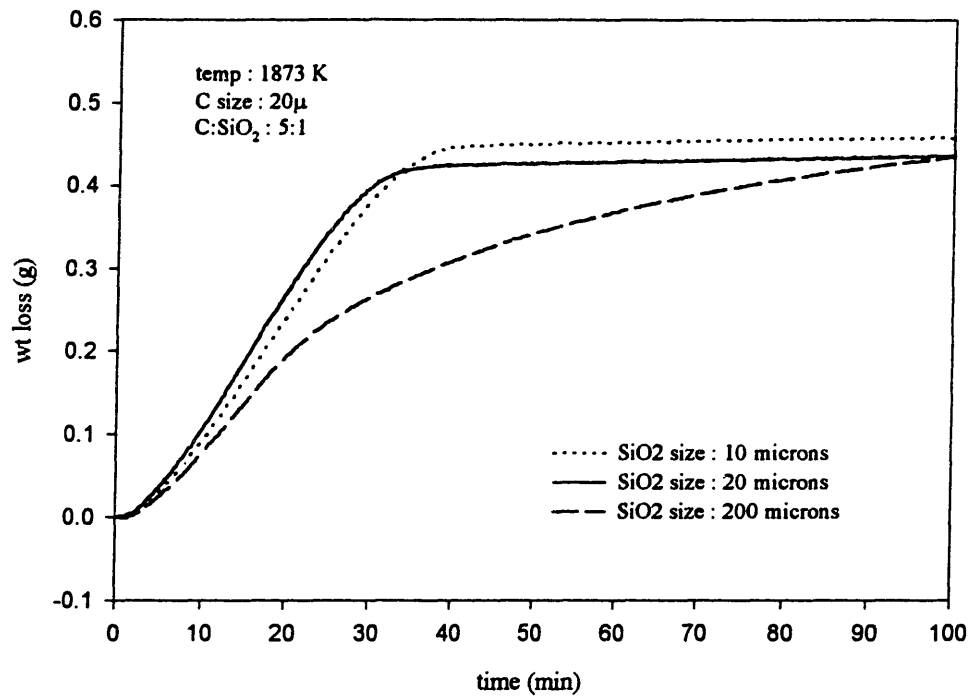


Figure 5.3 Effect of silica particle size on reaction kinetics.

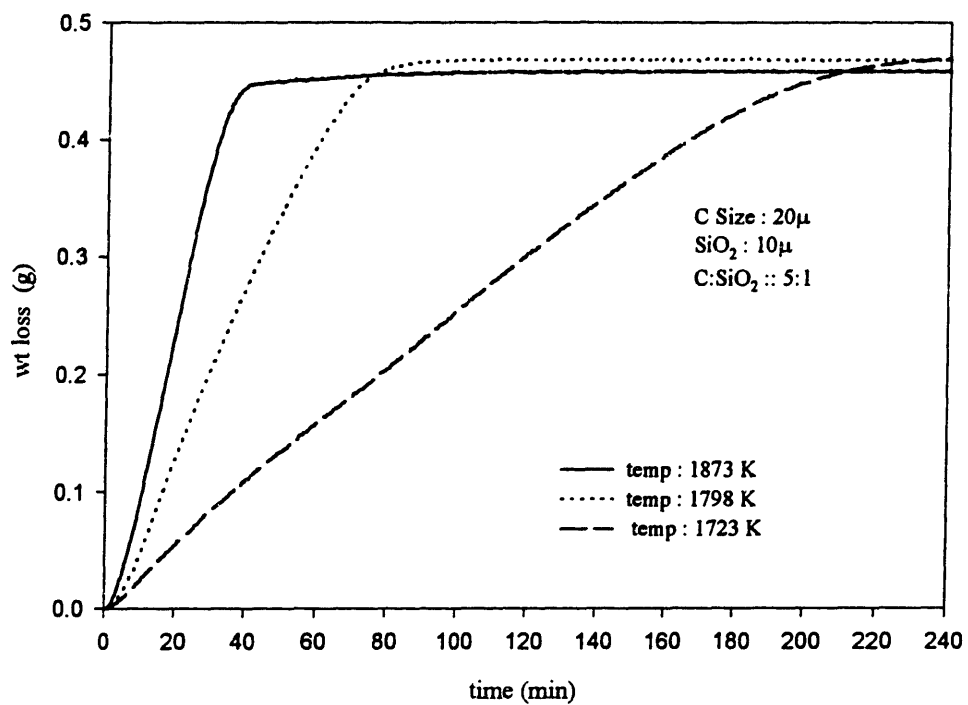


Figure 5.4 Effect of temperature on reaction kinetics.

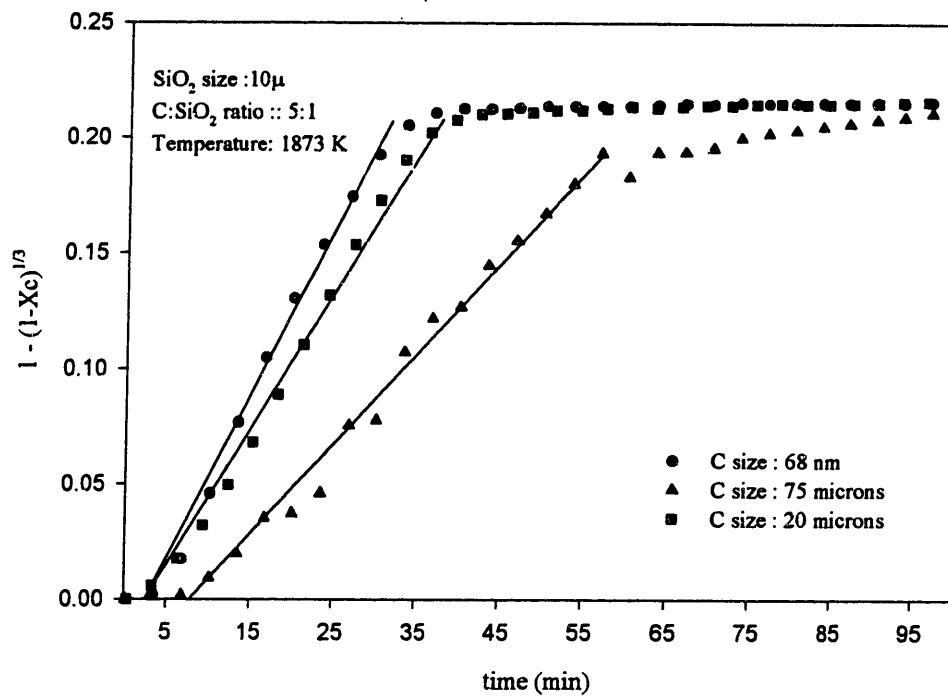


Figure 5.5 Surface reaction model for different carbon sizes.

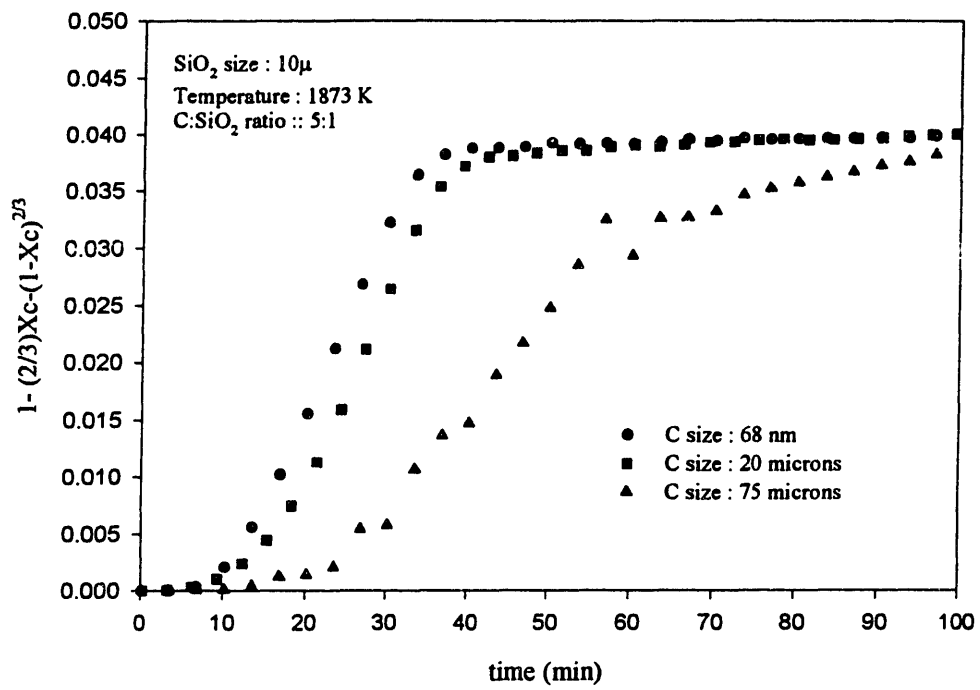


Figure 5.6 Ash layer model for different carbon sizes.

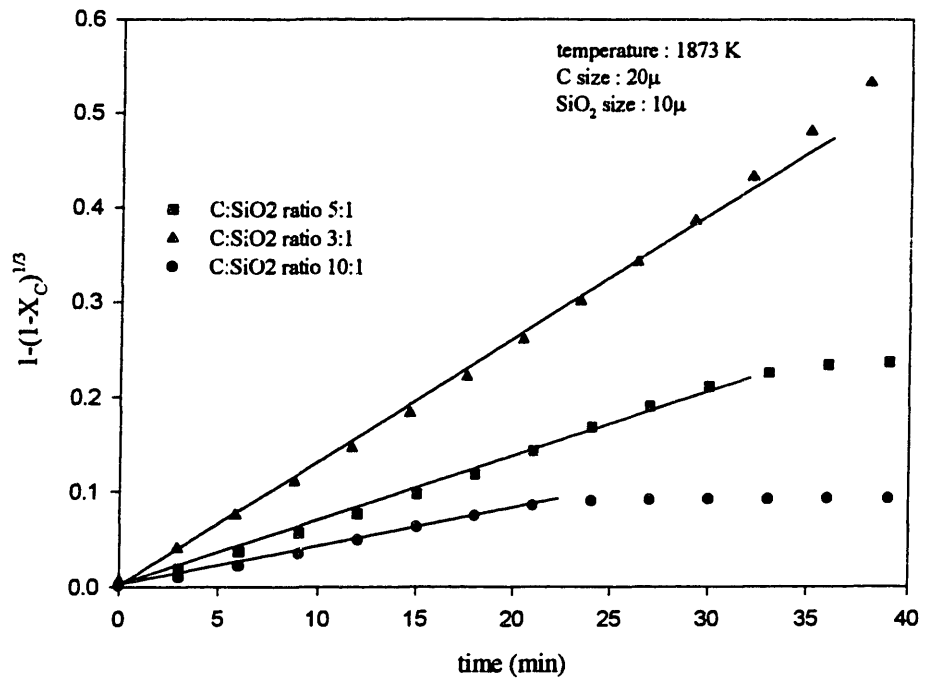


Figure 5.7 Surface reaction model for different C:SiO₂ ratios.

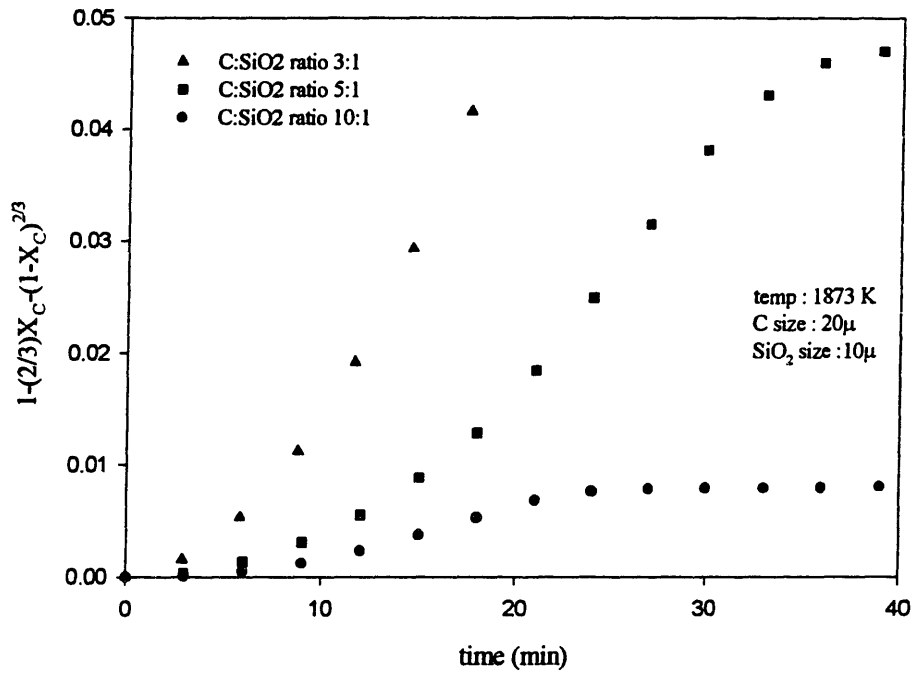


Figure 5.8 Ash layer model for different C:SiO₂ ratios.

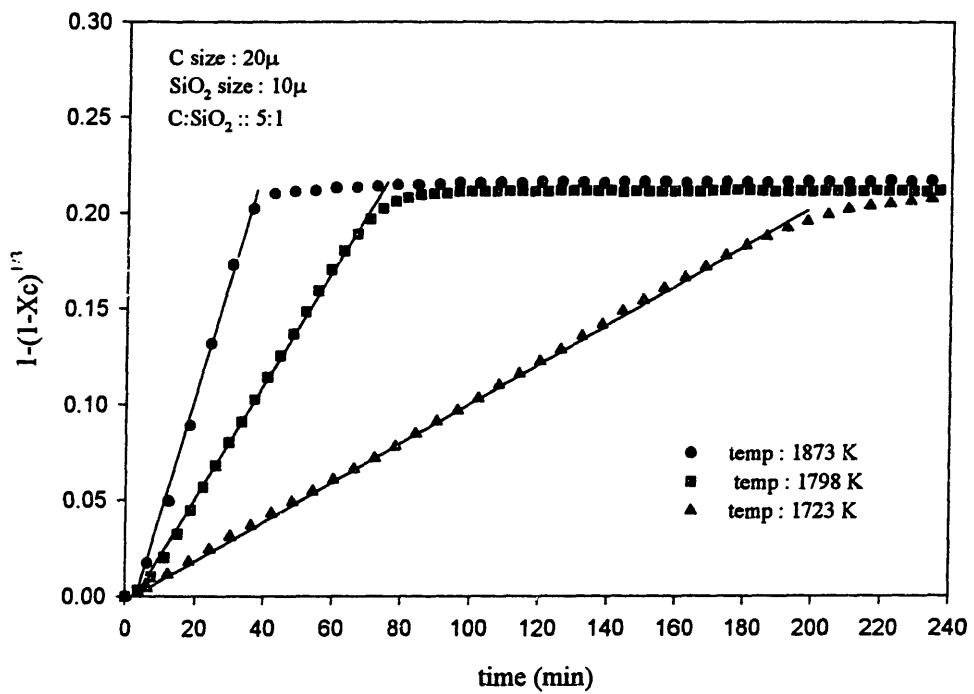


Figure 5.9 Surface reaction model for different temperatures.

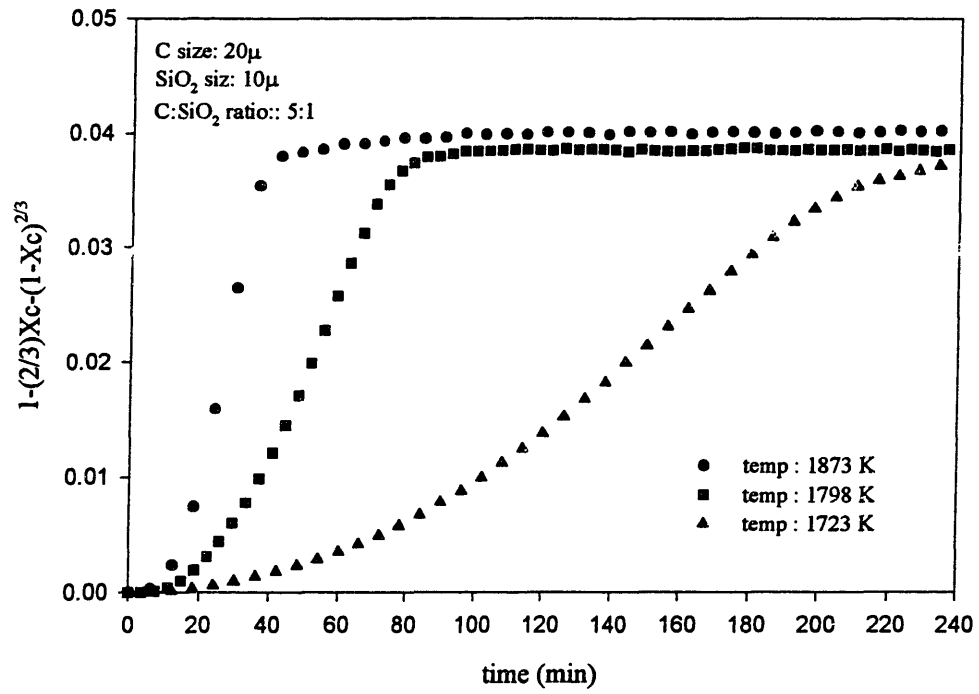


Figure 5.10 Ash layer model for different temperatures.

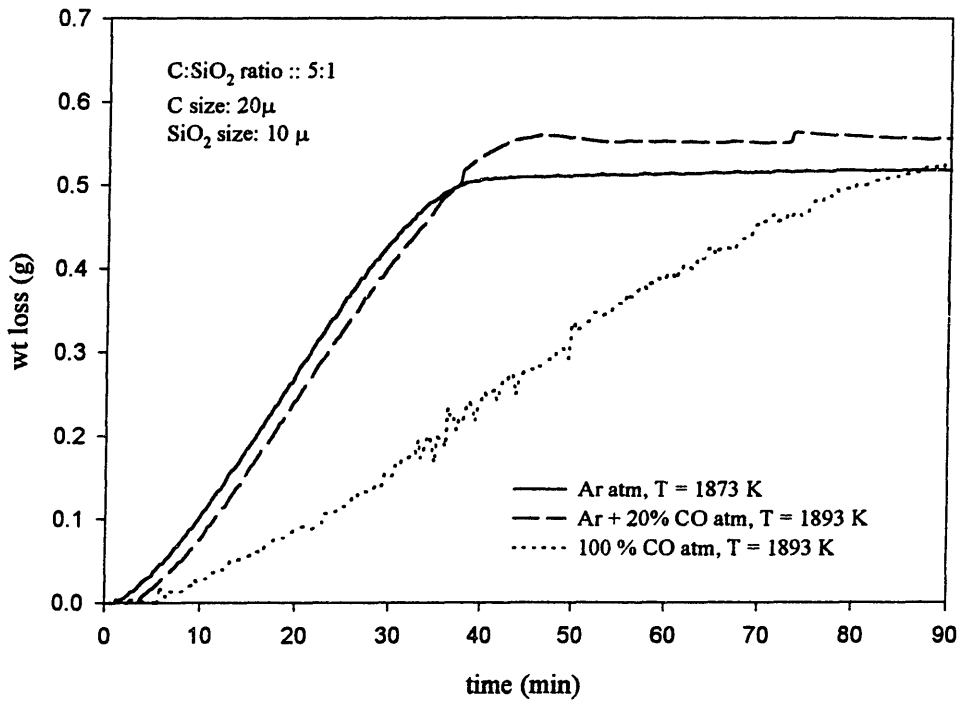


Figure 5.11 Effect of CO partial pressure in the surrounding atmosphere on the reaction kinetics.

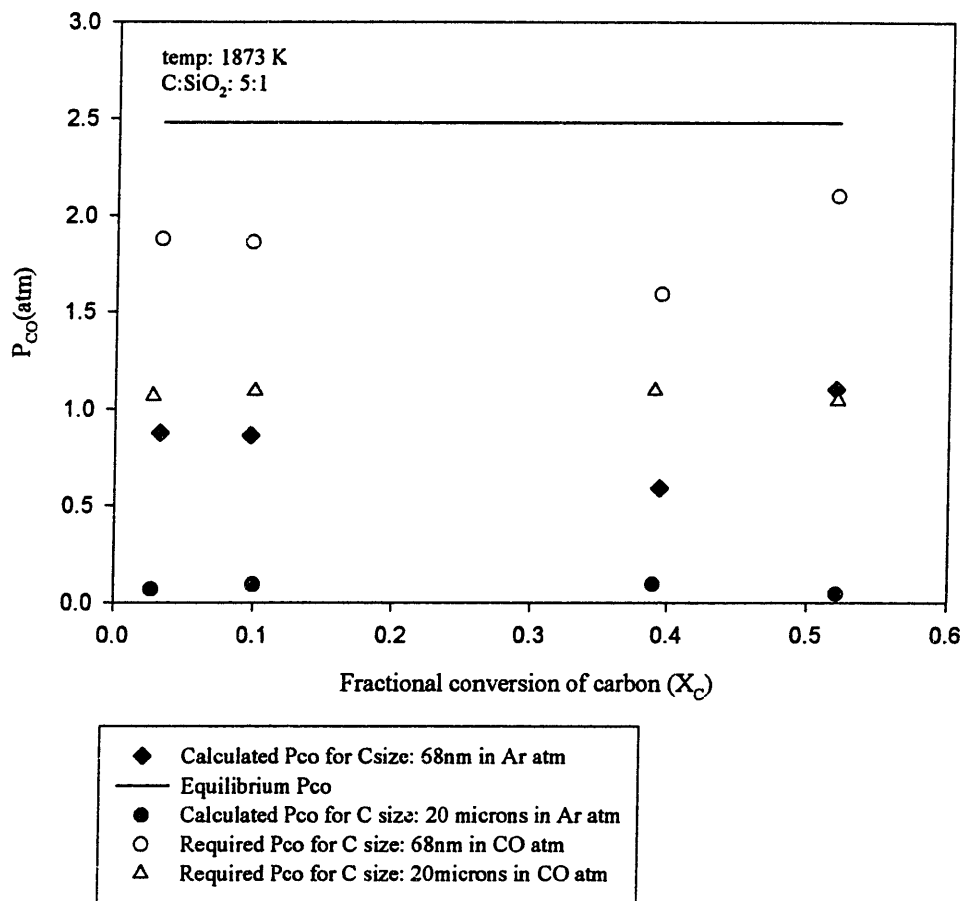


Figure 5.12 Estimation of the required CO pressures in the reaction pellet.

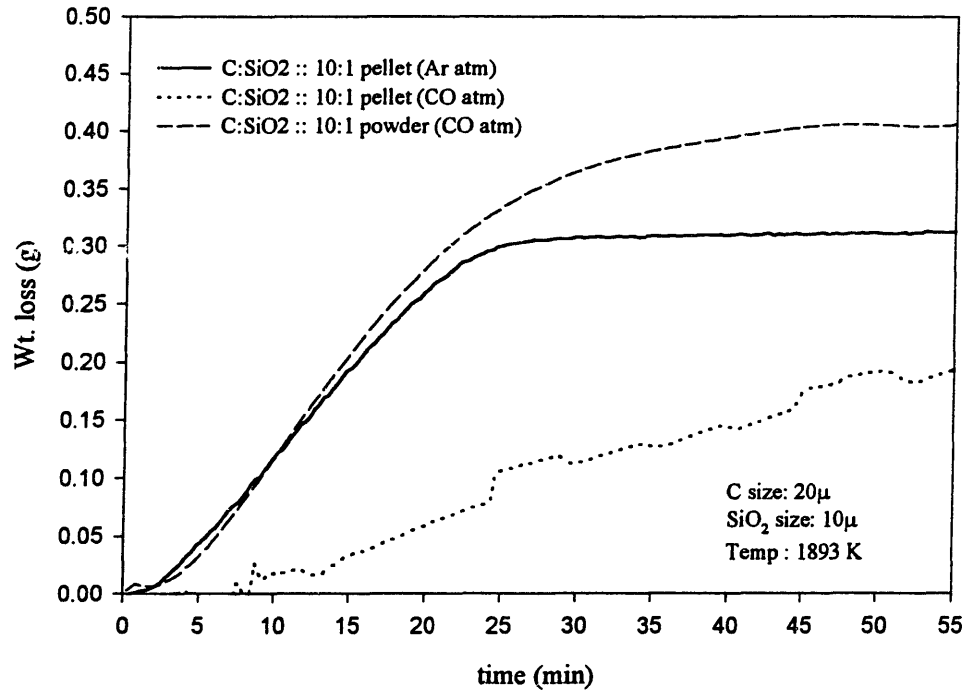


Figure 5.13 Effect of porosity on the reaction kinetics in presence of CO atmosphere.

Chapter 6

Mathematical Modeling

6.1 Introduction

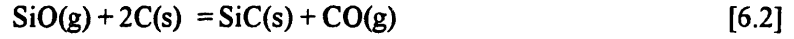
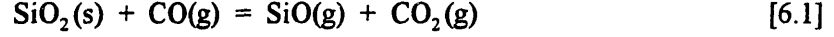
A mathematical model has been developed to represent the carbothermic reduction of silica. Experimental study described earlier yielded the parameters necessary to ensure that surface reaction is rate determining in the carbothermic reduction process. Theoretical analysis is necessary to gain a more fundamental understanding of the contribution of the individual reactions in the overall kinetics determined by the surface reactions. The model is an extension of the theoretical analysis done by Szekely et. al.^[13] for the case of solid-solid reactions proceeding through gaseous intermediates.

6.2 Development of the model

In the present study the following assumptions hold:

- 1) Particle size for the reactants is uniform and the particles are spherical in shape. The consideration of uniform particle size and idealized particle shape may be an oversimplification but it leads to an ease of analysis.
- 2) The overall rate of reaction is controlled by chemical kinetics, the concentration of the gaseous species is uniform throughout the pellet and diffusion of the gaseous reactants through the product layer of the individual particles is not rate limiting. This is established by the selection of the experimental parameters as described earlier.
- 3) The system is isothermal. This is established by having a large hot zone and small pellet size.

The key reactions in the carbothermic reduction process are:



The net rate at which the gaseous components are being generated may be calculated by subtracting their rate of consumption from the rate of generation. Net rates can then expressed as

$$\frac{dn_{\text{SiO}}}{dt} = v_1 - v_2 \quad [6.4]$$

$$\frac{dn_{\text{CO}}}{dt} = -v_1 + v_2 + 2v_3 \quad [6.5]$$

$$\frac{dn_{\text{CO}_2}}{dt} = v_1 - v_3 \quad [6.6]$$

where v_1 , v_2 and v_3 are the net forward rates of reactions [6.1], [6.2] and [6.3] respectively, per unit volume of the pellet and n is the number of moles of the gaseous species.

The advancement of reaction interface within the particle may be expressed as

$$\rho_s \frac{dr_s}{dt} = -k_1 C_{\text{CO}} \quad [6.7]$$

$$\rho_c \frac{dr_c}{dt} = -(2k_2 C_{\text{SiO}} + k_3 C_{\text{CO}_2}) \quad [6.8]$$

The reactions are assumed to be irreversible and of the first order in order to simplify the interpretation of the results. The k is the intrinsic rate constant, C is the chemical concentration of the gaseous species, r is the particle radius and ρ is the molar density of the reactant. Using equations [6.7]-[6.8] the net forward reaction rates may be expressed in terms of concentrations of the gaseous species in the following form:

$$v_1 = \alpha_s \left(\frac{A_s}{V_s} \right) \left(\frac{r_s}{R_s} \right)^2 k_1 C_{\text{CO}} \quad [6.9]$$

$$v_2 = \alpha_c \left(\frac{A_c}{V_c} \right) \left(\frac{r_c}{R_c} \right)^2 k_2 C_{SiO} \quad [6.10]$$

$$v_3 = \alpha_c \left(\frac{A_c}{V_c} \right) \left(\frac{r_c}{R_c} \right)^2 k_3 C_{CO_2} \quad [6.11]$$

where α_s and α_c are the volumes occupied by SiO_2 and C respectively, per unit volume of the pellet. The surface area and volume of unreacted grain are designated by A and V, respectively, and R is the initial radius.

In a constant-pressure system the following relationships hold^[13]:

$$\frac{1}{V_p} \frac{dV}{dt} = \frac{1}{C_{CO}} \frac{dn_{CO}}{dt} = \frac{1}{C_{CO_2}} \frac{dn_{CO_2}}{dt} = \frac{1}{C_{SiO}} \frac{dn_{SiO}}{dt} \quad [6.12]$$

where dV/dt is the rate of increase in volume of the gaseous mixture, and V_p the volume of the pellet. Here a pseudo steady-state assumption has been made that the gas-phase concentrations at any time are at the steady-state values corresponding to the amount and sizes of the solid at that time; i.e., $C dV/dt \gg VdC/dt$. We also have

$$C_{CO} + C_{SiO} + C_{CO_2} = C_T \quad [6.13]$$

where C_T is the total molar concentration of the gaseous species within the pellet.

Experimental determination of how each of the variables in the above equations will affect the reaction kinetics would be extremely difficult and time consuming. However, the variables above can be arranged into pertinent dimensionless groups that will reduce the amount of data necessary to describe the process of carbothermic reduction. Consider the following dimensionless quantities:

$$\begin{aligned} \Psi_{CO} &= C_{CO}/C_T, \quad \Psi_{CO_2} = C_{CO_2}/C_T, \quad \Psi_{SiO} = C_{SiO}/C_T, \\ \xi_c &= r_c/R_c, \quad \xi_s = r_s/R_s, \\ \gamma &= 2(\alpha_c/\alpha_s)\rho_c/\rho_s, \end{aligned}$$

$$\beta_2 = (\rho_s / \rho_c) \left(\frac{R_s}{R_c} \right) (k_2 / k_1),$$

$$\beta_3 = (\rho_s / \rho_c) \left(\frac{R_s}{R_c} \right) (k_3 / k_1),$$

$$t^* = \left(C_T k_1 / \rho_s R_s \right) t$$

Using these, the equations [6.4] – [6.15] can be reduced to the following dimensionless forms:

$$\frac{d\xi_s}{dt^*} = -\Psi_{CO} \quad [6.14]$$

$$\frac{d\xi_c}{dt^*} = -(2\beta_2 \Psi_{SiO} + \beta_3 \Psi_{CO_2}) \quad [6.15]$$

$$\gamma \beta_2 \left(\frac{\xi_c^2}{\xi_s^2} \right) \left(\frac{\Psi_{SiO}}{\Psi_{CO}} \right) = \frac{\Psi_{CO} + 2\Psi_{CO_2} - \Psi_{SiO}}{1 + \Psi_{CO_2}} \quad [6.16]$$

$$\gamma \beta_3 \left(\frac{\xi_c^2}{\xi_s^2} \right) \left(\frac{\Psi_{CO_2}}{\Psi_{CO}} \right) = \frac{\Psi_{CO} + \Psi_{SiO}}{1 + \Psi_{CO_2}} \quad [6.17]$$

$$\Psi_{SiO} + \Psi_{CO} + \Psi_{CO_2} = 1 \quad [6.18]$$

These dimensionless equations can be solved for the five unknown dimensionless quantities. Since the equilibrium partial pressure of CO(g) is very large compared to that of SiO(g) and CO₂(g) (fig. 4), Ψ_{CO_2} and Ψ_{SiO} are much smaller as compared to Ψ_{CO} . Therefore, by combining equations [6.16] and [6.17] we get

$$\beta_2 \Psi_{SiO} = \beta_3 \Psi_{CO_2} \quad [6.19]$$

6.3 Results and Discussion

Using Mathematica version 3.1, equations [6.16] – [6.18] were solved in the symbolic form to yield the following result:

$$\Psi_{SiO} = \frac{1}{2}(a + b + c - d) \quad [6.20]$$

$$\Psi_{CO_2} = \frac{1}{2}(2 - a - b - c + d + e - f) \quad [6.21]$$

$$\Psi_{CO} = \frac{1}{2}(f - e) \quad [6.22]$$

where

$$a = \frac{2\beta_2\beta_3}{(\beta_2 + \beta_3)^2} \quad [6.23]$$

$$b = \frac{2\beta_3^2}{(\beta_2 + \beta_3)^2} \quad [6.24]$$

$$c = \frac{\beta_2\beta_3^2\gamma\xi_c^2}{(\beta_2 + \beta_3)^2\xi_s^2} \quad [6.25]$$

$$d = \frac{\beta_2^{1/2}\beta_3^{3/2}\gamma^{1/2}\xi_c(\beta_2\beta_3\gamma\xi_c^2 + 4\beta_2\xi_s^2 + 4\beta_3\xi_s^2)^{1/2}}{(\beta_2 + \beta_3)^2\xi_s^2} \quad [6.26]$$

$$e = \frac{\beta_2\beta_3\gamma\xi_c^2}{(\beta_2 + \beta_3)\xi_s^2} \quad [6.27]$$

$$f = \frac{\beta_2^{1/2}\beta_3^{3/2}\gamma^{1/2}\xi_c(\beta_2\beta_3\gamma\xi_c^2 + 4\beta_2\xi_s^2 + 4\beta_3\xi_s^2)^{1/2}}{(\beta_2 + \beta_3)\xi_s^2} \quad [6.28]$$

In the studies conducted by Golovina^[14], Desai and Yang^[15] the intrinsic rate constant k_3 of the Boudouard reaction was found to be of the order of 10^{-2} cm/s. Fruehan et. al.^[7] in their study of the reaction of SiO(g) with carbon saturated iron measured the gas-phase mass transfer coefficient. The value was found to be of the order of 10^1 cm/sec. which indicates that the intrinsic rate constant k_2 for the reaction [6.2] is higher than this value Also, Fruehan et. al.^[16] studied the rate of formation of SiO(g) by the reaction of CO(g) with silica and they found the

intrinsic rate constant k_1 to be of the order of 10^{-2} to 10^{-3} cm/sec. Based on the available data mentioned above we can say that $\beta_2 \gg \beta_3$ and this indicates that reaction [6.2] is very fast as compared to reactions [6.1] and [6.3]. The above equations can therefore be simplified by assuming that $\beta_2/\beta_3 \rightarrow 0$. From equation [6.14] and [6.22] we have

$$\frac{d\xi_s}{dt^*} = \frac{\beta_3 \gamma \xi_c^2 - \xi_c \beta_3^{1/2} \gamma^{1/2} (\beta_3 \gamma \xi_c^2 + 4 \xi_s^2)^{1/2}}{2 \xi_s^2} \quad [6.29]$$

Also, from [6.15] and [6.19] - [6.20] we have

$$\frac{d\xi_c}{dt^*} = -3\beta_3 \left(1 + \frac{\beta_3 \gamma \xi_c^2 - \xi_c \beta_3^{1/2} \gamma^{1/2} (\beta_3 \gamma \xi_c^2 + 4 \xi_s^2)^{1/2}}{2 \xi_s^2} \right) \quad [6.30]$$

which can be expressed in the following manner:

$$\frac{d\xi_c}{dt^*} = -3\beta_3 \left(1 + \frac{d\xi_s}{dt^*} \right) \quad [6.31]$$

Integrating equation [6.31] between the limits 0 and t^* we can get a relationship between ξ_c and ξ_s of the form

$$\xi_s = -\frac{\xi_c - (1 + 3\beta_3) + 3\beta_3 t^*}{3\beta_3} \quad [6.32]$$

Substituting this in eq. [6.30] we get the following rate expression

$$\frac{d\xi_c}{dt^*} = -3\beta_3 \left[1 + \frac{9\beta_3^3 \gamma \xi_c^2 - (81\beta_3^6 \gamma^2 \xi_c^4 + 36\beta_3^3 \gamma \xi_c^2 (\xi_c - (1 + 3\beta_3) + 3\beta_3 t^*)^2)^{1/2}}{2(\xi_c - (1 + 3\beta_3) + 3\beta_3 t^*)^2} \right] \quad [6.33]$$

This non-linear differential equation was solved numerically to obtain the consumption rate of C as a function of time. Values of β_3 and γ were needed for this purpose. These variables also represent the input parameters in the reaction pellet. The value of γ represents the relative ratios of carbon and silica present in the pellet and β_3 can be calculated by knowing the values of particle radii, molar densities for carbon and silica and the intrinsic rate constants k_1 and k_3 . Since, different values for k_1 and k_3 have been quoted in the literature by different authors^[7,14-15], their orders of magnitude were considered and the values were adjusted to get a good fit with the experimental data maintaining their order of magnitude. Values of k_1 and k_3 thus found, were 0.003 cm/s and 0.04 cm/s respectively. Same values of these rate constants were used throughout the analysis.

Effect of carbon particle size

Figs.6.1 and 6.2 show the fractional conversion of carbon and silica respectively as a function of time for different sizes of carbon particles. We see a good match between the experimental and the theoretical data. This validates our assumption that surface reactions indeed are rate limiting. Reaction kinetics increases with decrease in the particle size of carbon. Below a certain critical size of the carbon particles the rate of conversion does not improve significantly. Boudouard reaction is faster than the reduction reaction of silica ($\beta_3 \sim 10.0$). By decreasing the particle size the Boudouard reaction can be enhanced but a stage comes when the net reaction is limited by the kinetics of reaction [6.1] and decreasing the particle size of carbon does not lead to an improvement in the reaction kinetics.

Effect of silica particle size

Reaction kinetics decrease with increase in the particle size of silica due to reduced surface area available for the reaction (figs. 6.3 and 6.4). Mismatch between the experimental data and theoretical results for starting silica size of 200 μ is probably due to a significant size reduction caused by milling (12 hrs). Again reducing the particle size of silica below a certain critical size would make the reaction kinetics for the reduction of silica comparable to that for the Boudouard reaction and as a result the reaction kinetics will not improve much.

Effect of C:SiO₂ ratio

The effect of the ratio of the starting materials can be observed from figs.6.5 and 6.6. Fractional conversion of carbon is dependent on the C:SiO₂ ratio of the starting pellet because of the excess carbon. This can be seen from fig.6.5. Thus a higher fractional conversion is achieved for the C:SiO₂ ratio of 5:1 as compared to 10:1. However, the reaction time remains the same as can be observed from the solid curves. Theoretically the conversion of silica should be unaffected by the starting ratio as shown by the overlapping curves for 5:1 and 10:1 starting ratios (fig 6.6). This is because the silica is almost completely consumed and the conversion is rate limited by surface reaction. However, experimental results vary to some extent. The possible reason for this is some rate limitation imposed by the diffusion of gaseous reactants through the porous SiC layer around the carbon particles for a C:SiO₂ ratio of 5:1 leading to a slightly higher reaction time.

It can be seen that the experimental results haven been successfully interpreted by using this model. Also it was possible to explain the contributions of the individual reactions to the overall kinetics of carbothermic reduction and thereby gain a more fundamental understanding of the reduction process. It is possible to further improve the model predictions by conducting separate experimental studies to determine the values of the reaction constants and their dependency on the temperature.

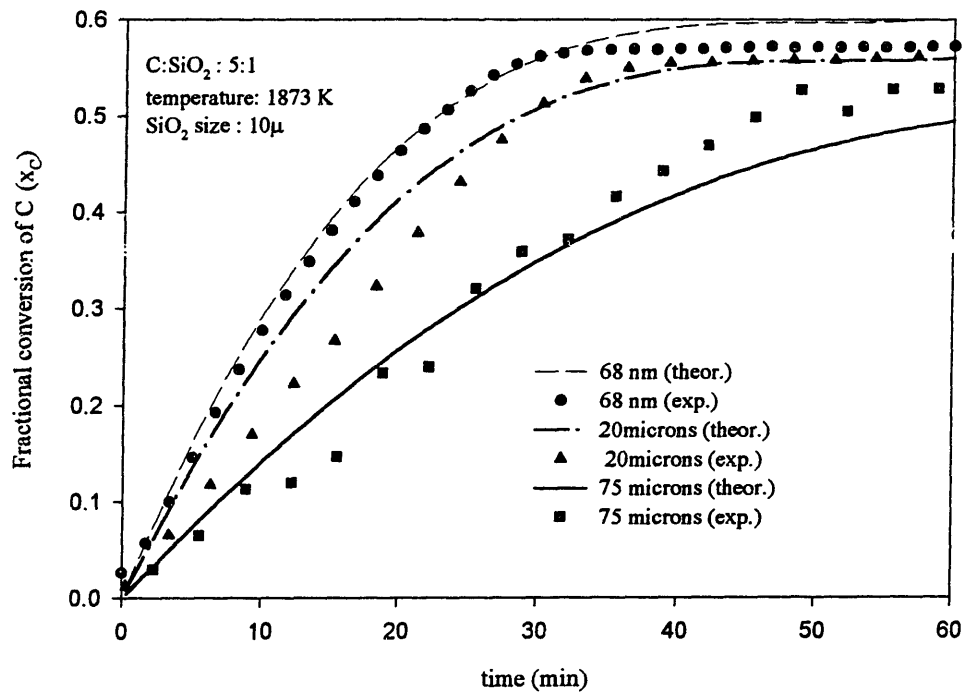


Figure 6.1 Fractional conversion of carbon as a function of time for different carbon particle sizes.

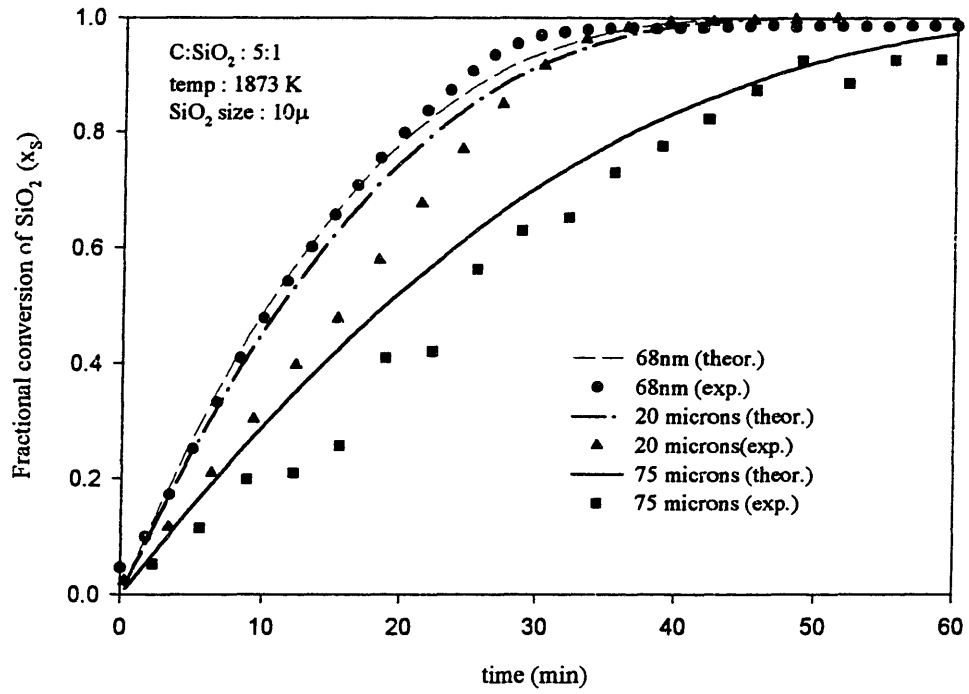


Figure 6.2 Fractional conversion of silica as a function of time for different carbon particle sizes.

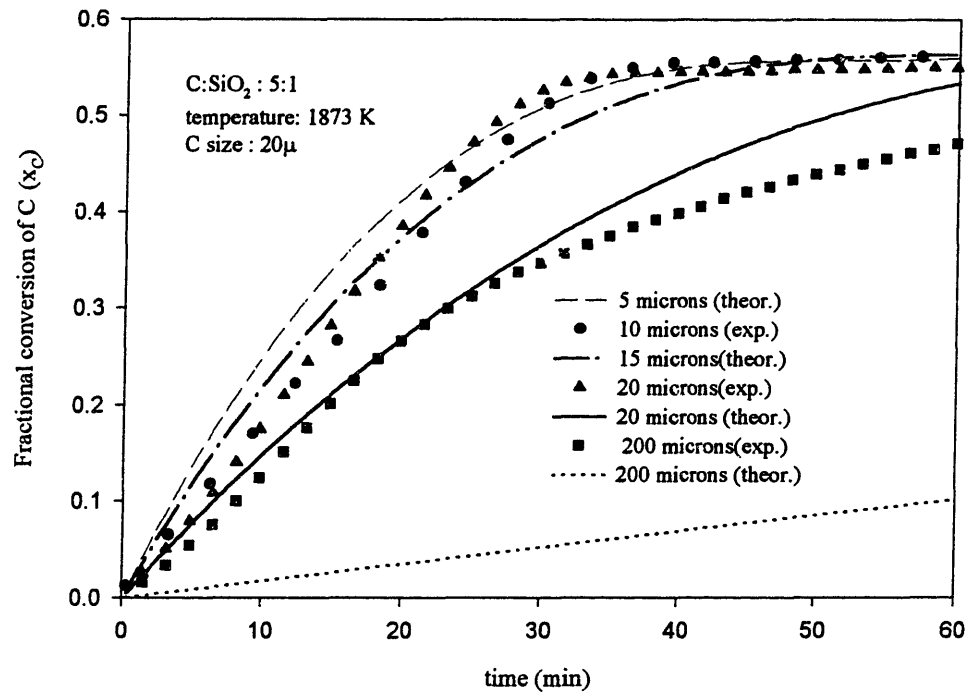


Figure 6.3 Fractional conversion of carbon as a function of time for different silica particle sizes.

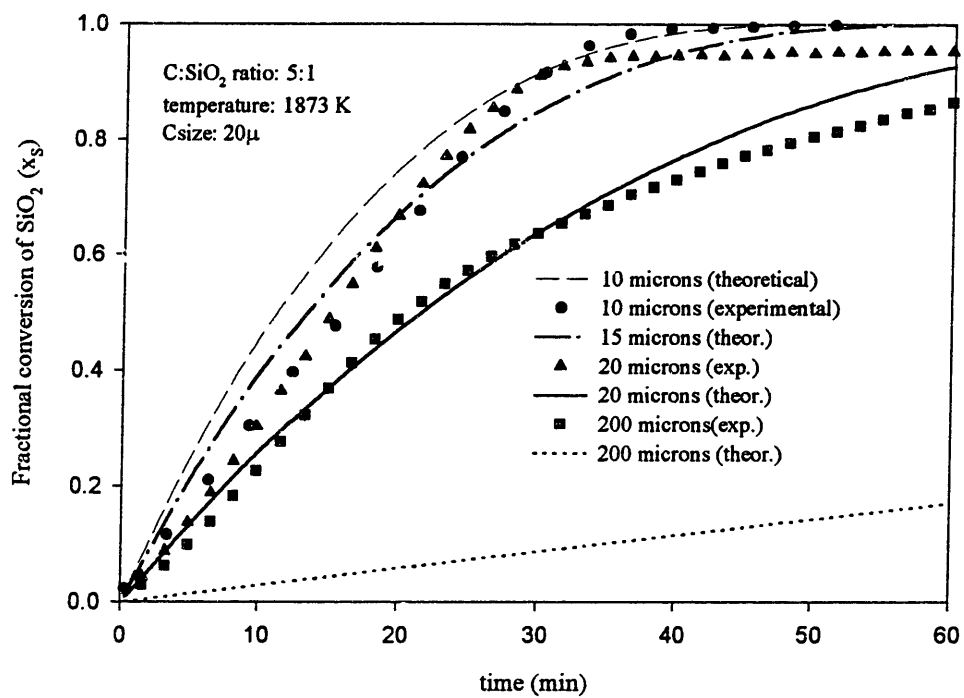


Figure 6.4 Fractional conversion of silica as a function of time for different particle sizes.

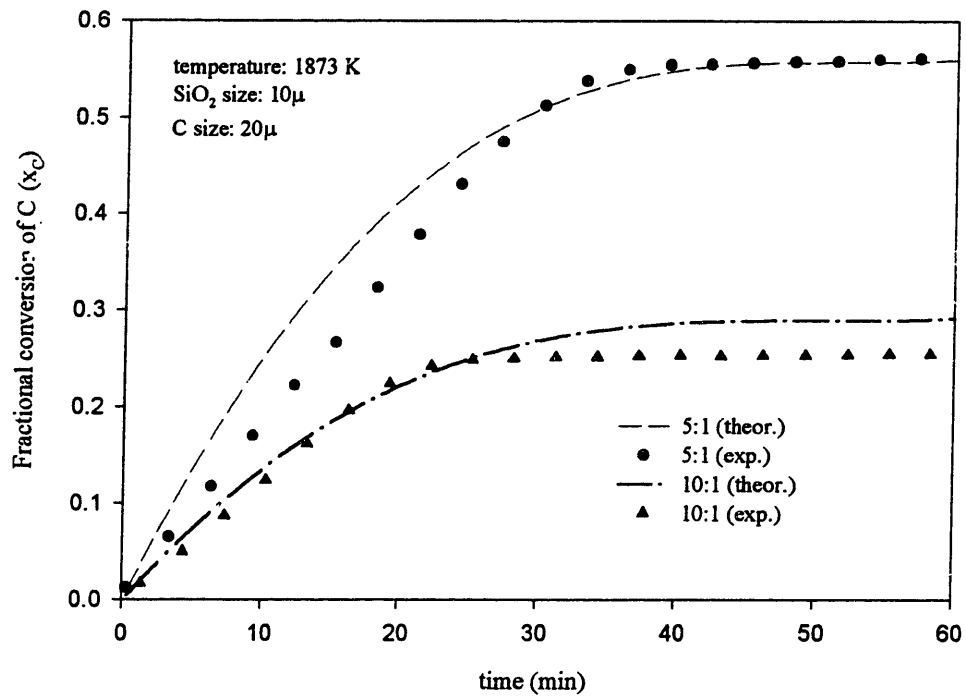


Figure 6.5 Fractional conversion of carbon as a function of time for different C:SiO₂ ratios.

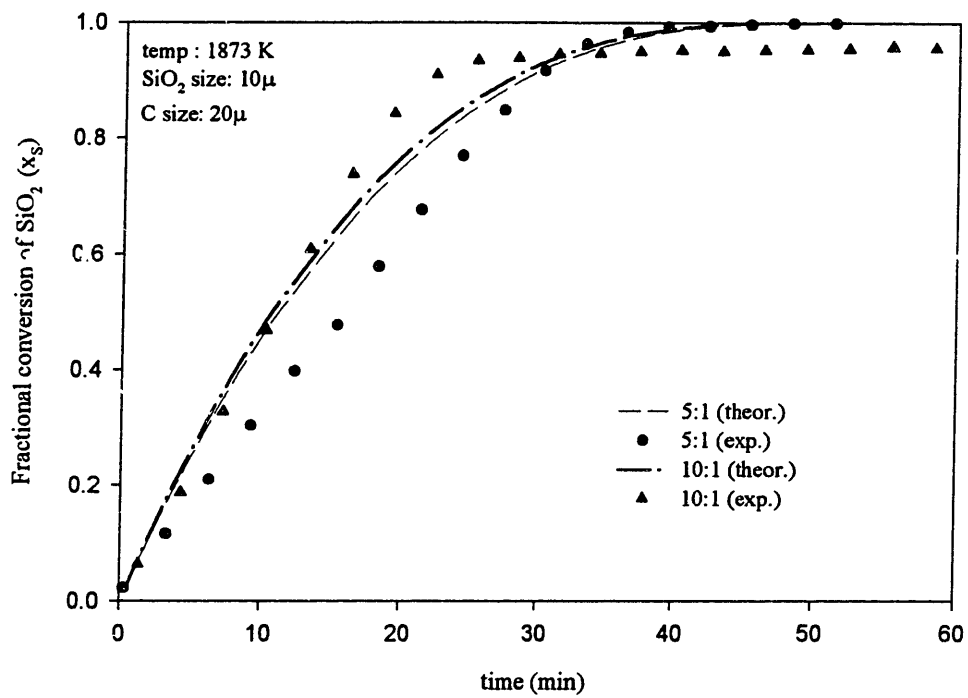


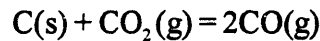
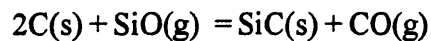
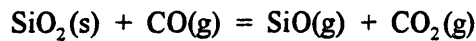
Figure 6.6 Fractional conversion of silica as a function of time for different C:SiO₂ ratios.

Chapter 7

Conclusions

Following conclusions can be drawn from this study:

1) Carbothermic reduction of silica at temperatures above 1773 K is a composite reaction and the possible mechanism involves the following three gas solid reactions:



2) For C:SiO₂ ratios (>5:1) with carbon particle size less than 75μ and silica size less than 20μ in the form of pellets pressed at 9000 psi, surface reaction is the dominant rate determining step and diffusion of reactants through the porous SiC layer that forms on the carbon surface is not rate limiting. For larger particle sizes higher ratios may be needed for surface reaction control.

3) Reaction rate is controlled by the combination of silica reduction reaction and the Boudouard reaction.

4) Reaction kinetics increases with decrease in the particle size of silica as well as carbon due to increase in the available surface area for silica reduction and Boudouard reactions to occur. However, significant size reductions of either carbon or silica lead the other reaction to become rate determining and as a result the kinetics improves only marginally. Reaction kinetics is more sensitive to the silica particle size due to low reaction constant of the reduction reaction of silica.

5) Overall reaction kinetics can be tailored through a proper selection of carbon to silica ratio, their particle sizes and compaction pressure of the pellet to ensure in-situ carbothermic reduction of silica and as a result ferro-silicon alloys can be suitably synthesized using this alternate approach.

Nomenclature

A_x	surface area of the unreacted particle of solid x (m^2)
C_g	molar concentration of species g ($mol\ m^{-3}$)
C_T	total molar concentration of gaseous species within the pellet ($mol\ m^{-3}$)
D_{eff-CO}	effective diffusivity of CO(g) ($m^2\ s^{-1}$)
g	gaseous species CO, CO ₂ and SiO
K_1	constant for surface reaction control dimensionally representing the intrinsic rate constant (ms^{-1})
K_2	constant for ash layer control dimensionally representing the diffusivity of the gaseous species ($m^2\ s^{-1}$)
k_1	intrinsic rate constant of reaction [5] ($m\ s^{-1}$)
k_2	intrinsic rate constant of reaction [6] ($m\ s^{-1}$)
k_3	intrinsic rate constant of reaction [12] ($m\ s^{-1}$)
L	half thickness of the sample pellet (m)
n_x	moles of species x (mol)
r_x	radius of the unreacted particle of solid x (m)
R_x	initial particles radius of solid x (m)
R	gas constant ($J\ mol^{-1}\ K^{-1}$)
S_0	particle surface area per unit volume of the solid (m^{-1}).
t	time (s)
T	temperature (K)
V	volume of the gaseous mixture (m^3)
v_i	net forward rate of reaction i per unit volume of the pellet ($mol\ m^{-3}\ s^{-1}$)
\bar{V}_0	flow velocity of CO gas ($m\ s^{-1}$)
V_p	volume of the pellet (m^3)
V_x	volume of the unreacted particle of solid x (m^3)
x	solid species C and SiO ₂
X_C	Fractional conversion of carbon
α_x	volume occupied by species x per unit volume of the pellet (m^3)
ΔP	pressure difference between the pellet interior and the atmosphere

ΔP_{CO}	CO pressure difference between the pellet interior and the atmosphere
ε	porosity of the pellet
η_{CO}	viscosity of the CO gas
ρ_{CO}	molar density of CO(g) (mol m^{-3})
τ	tortuosity of the pellet

Bibliography

1. R. Elliott: *Cast Iron Technology*, Butterworths, London, 1988, p-74.
2. B. Ozturk and R.J. Fruehan: *Metall. Trans. B*, 1985, vol. 16B, pp. 121-27.
3. J.G. Lee and I.B. Cutler: *Am. Ceram. Soc. Bull.*, 1975, vol. 54, No.2, pp. 195-98.
4. J.J. Biernacki and G.P. Wozak: *Journal of Thermal Analysis*, 1989, vol. 55, pp. 1651-67.
5. T. Shimoo, F. Mizutaki, S. Ando, H. Kimura: *J. Japan Inst. Metals*, 1988, vol. 52, No. 10, pp. 945-53.
6. V. D. Krstic: *J. Am. Ceram. Soc.*, 1992, vol. 75, No. 1, pp. 170-174.
7. A. Roine: *HSC Chemistry for Windows*, version 2.0, Outokumpu Research, Finland, 1994, pp 35-47.
8. O. Levenspiel: *Chemical Reaction Engineering*, 2nd ed., John Wiley & Sons, New York, 1972, pp. 357-408.
9. G.H. Geiger and D.R. Poirier: *Transport Phenomena in Materials Processing*, The Minerals, Metals & Materials Society, Warrendale, PA, pp. 93-101.
10. W.J. Rankin and J.R. Wynnyckyj: *Metall. Trans. B*, 1997, vol. 28B, pp. 307-19.
11. J. Szekely, J.W. Evans and H.Y. Sohn: *Gas-Solid Reactions*, Academic Press, New York, NY, 1976, pp. 23-33.
12. N. Wakao and S. Kaguei: *Heat and Mass Transfer in Packed Beds*, Gordon and Breach, New York, NY, 1982, pp. 114-37.
13. J. Szekely, J.W. Evans and H.Y. Sohn: *Gas-Solid Reactions*, Academic Press, New York, NY, 1976, pp. 176-204.
14. E.S. Golovina: *Carbon*, 1980, vol. 18, pp. 197-201.
15. N.J. Desai and R.T. Yang: *AIChE Journal*, 1982, vol. 28, No. 2, pp. 237-244.
16. B. Ozturk and R.J. Fruehan: *Metall. Trans. B*, 1985, vol. 16B, pp. 801-806.

Biographical Note

The author was born on May 12, 1998 in Pune, India. He graduated from the Indian Institute of Technology, Bombay in June 1996, with the degree of Bachelor of Technology in Metallurgical Engineering and Materials Science. He came to the Massachusetts Institute of Technology as a graduate student in the Department of Materials Science and Engineering in July, 1996.

The author is a member of The Minerals, Metals and Materials Society, ASM International and The American Ceramic Society.